

LaDP-FL: Local Layer-wise Differential Privacy in Federated Learning

Yunbo Li, *Student Member, IEEE*, Jiaping Gui, *Member, IEEE*, Fanchao Meng, Yue Wu, *Senior Member, IEEE*

Abstract—Federated Learning (FL) enables collaborative model training without direct data sharing, yet it remains vulnerable to privacy attacks such as model inversion and membership inference. Existing differential privacy (DP) solutions for FL often inject noise uniformly across the entire model, degrading utility while providing suboptimal privacy-utility tradeoffs. To address this, we propose LaDP-FL, a novel layer-wise adaptive noise injection mechanism for FL that optimizes privacy protection while preserving model accuracy. LaDP-FL leverages two key insights: (1) neural network layers contribute unevenly to model utility, and (2) layer-wise privacy leakage can be quantified via KL divergence between local and global model distributions. LaDP-FL dynamically injects noise into selected layers based on their privacy sensitivity and importance to model performance.

We provide a rigorous theoretical analysis, proving that LaDP-FL satisfies (ϵ, δ) -DP guarantees and converges under bounded noise. Extensive experiments on CIFAR-10/100 datasets demonstrate that LaDP-FL reduces noise injection by 46.14% on average compared to state-of-the-art (SOTA) methods while improving accuracy by 102.99%. Under the same privacy budget, LaDP-FL outperforms SOTA solutions like Dynamic Privacy Allocation LDP and AdapLDP by 25.18% and 6.1% in accuracy, respectively. Additionally, LaDP-FL robustly defends against reconstruction attacks, increasing the FID of the reconstructed private data by >12.84% compared to all baselines. Our work advances the practical deployment of privacy-preserving FL with minimal utility loss.

Index Terms—Federated Learning, Differential Privacy, Model Inverse Attack, Layer-grained.

I. INTRODUCTION

FEDERATED learning (FL) [1] has become a paradigm for collaborative machine learning, which enables participants to exchange model parameters or gradient updates without directly sharing their private data with a central aggregating server. With the capability of preserving participant privacy and addressing the issue of data isolation, FL has attracted substantial interest from researchers in recent years [2]–[4]. However, FL systems encounter practical challenges in providing comprehensive privacy protection for all participants to prevent various privacy attacks, such as deep leakage from gradients [5], [6], source inference attacks [7], [8], model inversion attacks [9], [10], and membership inference attacks [11], [12]. Consequently, the private data of participants remains a significant privacy risk.

To mitigate the aforementioned privacy concerns, researchers have proposed different solutions that can be categorized into two types of mechanisms: homomorphic encryption

Yunbo Li, Jiaping Gui, Fanchao Meng, and Yue Wu are with Shanghai Jiao Tong University, Shanghai, 200240, China (e-mail: {li-yun-bo, jgui, mactavishmeng, wuyue}@sjtu.edu.cn).

(HE) [13], [14] and differential privacy (DP) [15], [16]. HE is a technique that encrypts the plaintext and ensures that the result of performing operations on the ciphertext is equivalent to that of performing corresponding operations on the plaintext. Through encryption, this mechanism effectively prevents malicious servers from intercepting or stealing model information during transmission. However, HE can incur significant resource overhead [17], which limits its application in the real world. In contrast, DP prevents adversaries from inferring private model information by rendering neighboring datasets indistinguishable. Specifically, DP introduces constrained noise to model parameters and then obfuscates them. A typical method to implement DP in FL is to inject noise into local models, also known as local differential private federated learning (LDP-FL) [16], [18]. Despite the promise to protect the privacy of each participant, LDP-FL may significantly impair the performance of the global model [15] since the noise is accumulated on the server side.

Extensive research [17]–[21] has been conducted to find an optimal trade-off between the privacy protection of local models and the inference performance of the global model in LDP-FL. To achieve this, researchers have designed various adaptive strategies to dynamically adjust the amount of noise injection, leveraging model information such as \mathcal{L}_2 norm [21], clip bound [20], sensitivity [17], and propagation errors [22]. This information is determined by comparing the current training round with historical round(s). However, existing approaches estimate privacy guarantees for the entire local model during each iteration, which results in unnecessary noise addition to layers that contain minimal or no private information but are crucial for prediction accuracy. Consequently, the performance of the global model degrades.

To address the aforementioned limitations, we propose LaDP-FL, a novel privacy protection approach in FL that leverages layer-wise noise injection in local models. A key insight in LaDP-FL is that neural network layers impose varying degrees of impact (i.e., importance) on the global model [23]–[25]. Besides, these layers, providing granular details of local models, can be manipulated independently [26], [27]. Unlike existing works that solely support noise injection across the entire local model, LaDP-FL can selectively identify neural network layers based on their importance and inject varying levels of noise into these layers to protect privacy.

However, fulfilling the above insights presents two challenges. First, how to inject noise into selective neural network layers to protect privacy while maintaining model accuracy is an open problem. An ideal solution is to inject more noise in layers that contain significant private information but have

a relatively small impact on the model’s accuracy. However, this is a challenging task pertaining to model interpretability, especially in complex neural network structures. Second, each participant lacks prior knowledge about the optimization direction of the global model. It is difficult to determine the noise injection amount for different layers in a local model.

To tackle the first challenge, LaDP-FL leverages a Layer Selection module to determine the importance of each local neural network layer on the global model. Specifically, this module utilizes the weight values of each layer as an indicator of its influence on the inference accuracy of the global model. We adopt this strategy because adversaries rely on the predictive capabilities of the global model to launch attacks by training shadow models (e.g., binary classifiers used in membership inference attacks [11], [28] or the GANs used in model inversion attacks [9], [10]). If layers within a local model harbor private information yet exert little or no impact on the global model’s accuracy, adversaries would face difficulties in training a shadow model that facilitates their attack. To handle the second challenge, LaDP-FL employs a Privacy Estimation module that adopts a carefully crafted Kullback-Leibler (KL) divergence-based approach to estimate the amount of private information contained in each layer of the local model. This amount serves as a crucial indicator to quantify the privacy levels of critical layers, guiding the subsequent layer-wise noise injection. We demonstrate that by dynamically injecting noise into selected neural network layers, LaDP-FL achieves an optimal balance between privacy protection and model accuracy.

In addition, we provide a thorough theoretical analysis of the privacy and convergence properties of LaDP-FL. Specifically, we derive bounds on the parameters that ensure differential privacy guarantees of LaDP-FL within Gaussian mechanisms. Under smoothness assumptions, we establish upper bounds on the model’s convergence. Our theoretical analysis reveals that, under specific conditions, LaDP-FL approaches the theoretical optimal upper bound as the iteration number increases, thereby providing a rigorous guarantee of its asymptotic optimality.

We conducted a comprehensive evaluation on the efficacy of LaDP-FL utilizing the ResNet-18 [29] and CNN architecture on two prominent datasets: CIFAR-10 [30] and CIFAR-100 [30]. We rigorously evaluated LaDP-FL in terms of accuracy, noise injection scale, and resource utilization under various scenarios. Experimental results demonstrate that, when compared to the traditional Gaussian DP mechanism (Full DP) [31], Time-Varying DP [18], and Sensitive DP [17], LaDP-FL reduces the average noise injection amount by 69.32%, 51.35%, and 1.2%, respectively, while the model accuracy increases by 236.32%, 144.93%, and 102.42%, respectively. Meanwhile, under the same privacy budget, LaDP-FL outperforms two state-of-the-art (SOTA) solutions, Dynamic Privacy Allocation LDP [32] and AdapLDP [33], by an average of 25.18% and 6.1%, respectively, in terms of accuracy. Additionally, LaDP-FL injects an average of 40.54% and 68.31% less noise than Dynamic Privacy Allocation LDP and AdapLDP, respectively. By averaging these results, it can be concluded that LaDP-FL achieves an average accuracy improvement of 102.99% across all scenarios, as well as

a reduction in average noise injection by 46.14%. Overall, LaDP-FL achieves a superior balance between privacy protection and model accuracy with a feasible time cost. To verify the privacy protection capability of LaDP-FL, we further validated its resistance against image reconstruction attacks on FEMNIST [34] and CIFAR-10 [30] datasets. The results show that attackers can hardly infer the victim’s private data after utilizing LaDP-FL’s strategy.

We summarize our contributions as follows:

- **Layer-wise Privacy Protection Framework.** We propose LaDP-FL, the first federated learning framework that provides differential privacy guarantees through adaptive layer-wise noise injection. By selectively perturbing critical neural network layers, LaDP-FL achieves finer-grained privacy-utility tradeoffs compared to model-level DP approaches.
- **Dynamic Privacy Estimation.** We design a novel KL-divergence-based module to quantify layer-specific privacy risks, enabling adaptive noise scaling proportional to the sensitive information contained in each layer. This addresses the limitations of coarse-grained with static/dynamic noise injection in prior work.
- **Theoretical Guarantees.** We formally prove that LaDP-FL satisfies (ϵ, δ) -DP under Gaussian mechanisms (Theorem 3). Furthermore, we establish convergence guarantees under non-IID data distributions (Theorem 4), demonstrating asymptotic optimality.
- **Comprehensive Evaluation.** We evaluate LaDP-FL on multiple datasets (CIFAR-10/100) and models (CNN, ResNet-18), showing: (1) *Accuracy*: 102.99% average improvement over SOTA DP-FL methods. (2) *Efficiency*: 46.14% reduction in noise injection volume. (3) *Robustness*: Effective defense against privacy reconstruction attacks. (4) *Scalability*: Maintains effectiveness under extreme non-IID settings.

Open Science. We release the source code of this project at <https://anonymous.4open.science/r/LaDP-92D7>.

II. RELATED WORKS

Utilizing DP for privacy protection in FL encompasses two primary research directions: Central Differential Privacy Federated Learning (CDP-FL) and Local Differential Privacy Federated Learning (LDP-FL). In this section, we will provide a comprehensive overview of the related work on both directions, including their distinct characteristics and design considerations.

A. Central Differential Privacy Federated Learning.

There are several works [35]–[37] that apply DP techniques by injecting noise on the server side. In such FL settings, the server injects noise into the model after aggregating new local models from all clients and then sends out the updated model to all clients. CDP-FL prevents participants from inferring each other’s information by disrupting the model distribution. In addition, CDP-FL poses minimum interference on the global model, thereby preserving its prediction performance. However, CDP-FL does not prevent the server from inferring

private information from local models [17] since the server can directly access client model weights or gradient parameters without any obfuscation. In contrast, our work primarily employs a local noise injection technique, which provides stronger privacy protection capabilities and ensures that local models cannot be analyzed by the server.

B. Local Differential Privacy Federated Learning.

Compared to CDP-FL, LDP-FL offers a safer protection mechanism and has garnered more extensive research attention [38]–[40], spanning fields such as wireless communication [41] and medical analysis [42]. Several studies [43], [44] have adopted a “first-compression-then-perturbation” approach, which reduces communication overhead while decreasing the dimensionality of noise injection. Chen *et al.* [45] further consider privacy allocation among different parties within compression. Yang *et al.* [46] focus on the personalized federated learning framework and inject noise only on shared parameters by utilizing Fisher information. However, all these approaches inject noise with a fixed distribution into their models. Over multiple iterations, excessive noise may be introduced, resulting in an increased signal-to-noise ratio within the model and subsequently impeding its performance.

To address this issue, researchers have explored methods for dynamically controlling noise injection quantities in each round to achieve a better privacy-utility tradeoff [18], [21], [32], [47]. Some works [17], [48] adjust noise scales by gradient clipping boundaries or historical model information. Fu *et al.* [20] propose Adap DP-FL, which injects noise into local gradients with adaptive scale adjustment, through clipping-bound updates based on previous bounds and model evolution. Lin *et al.* [49] introduce HDP-FL, which leverages contracts to incentivize each client to obtain the optimal amount of private data and more accurately inject dynamic noise. All these works adopt a coarse-grained approach, treating local neural network models as a single entity and injecting noise at the model level. However, this can lead to substantial performance degradation of the global model. In contrast, we propose injecting noise with finer granularity, which better balances model accuracy and privacy protection.

III. BACKGROUND

A. Federated Learning

FL systems typically consist of an aggregation server and multiple clients. Let S denote the aggregation server and $\mathcal{C} = \{\mathcal{C}_1, \mathcal{C}_2, \dots, \mathcal{C}_N\}$ denote N clients, each of which has a corresponding dataset \mathcal{D}_i , where $i \in \{1, 2, \dots, N\}$. Each data point $k \in \mathcal{D}_i$ is denoted by (x_k, y_k) . The server has a global model with weights denoted as w_g and a collection \mathcal{S} that stores all the data the clients upload. Furthermore, we use w_i^t to denote the local model parameters and $F(w_i^t)$ to represent the empirical risk function of the model in \mathcal{C}_i at the t^{th} global round. Therefore, \mathcal{C}_i can use a prediction loss function l to train its local model as:

$$\min_{w_i} F(w_i^t) \triangleq \frac{1}{|\mathcal{D}_i|} \sum_{k \in \mathcal{D}_i} l(k; w_i^t) = \frac{1}{|\mathcal{D}_i|} \sum_{k \in \mathcal{D}_i} l(y_k, w_i^t(x_k)). \quad (1)$$

The above loss function is typically optimized using the local stochastic gradient descent (SGD) algorithm as:

$$w_{i,e} = w_{i,e-1} - \eta \nabla F(w_{i,e-1}), \quad (2)$$

where e denotes the local training epoch and η is the learning rate. Note that we follow the same format as SCAFFOLD [2] to represent the local epoch (e.g., e in Equation 2) and global round (e.g., t in Equation 1).

In synchronous federated learning (SFL), the server employs a randomized selection process to determine a set of active clients, denoted by $\mathcal{AC} \subseteq \mathcal{C}$. Subsequently, all the activated clients upload their local models after completing local training. While the server receives shared data from all clients in \mathcal{AC} , it will update the global model [1] by:

$$w_g^t = \frac{1}{D} \sum_{w_i \in \mathcal{S}} |\mathcal{D}_i| w_i^t, \quad D \triangleq \sum_{w_i^t \in \mathcal{S}} |\mathcal{D}_i|. \quad (3)$$

B. Differential Privacy

DP quantifies the degree of divergence between two neighboring data points within a dataset, indicating the adversary’s capability to discern the data points based on the disclosed information. Based on this concept, we can establish a mathematical benchmark for assessing the privacy of a dataset.

Definition 1 $((\epsilon, \delta)\text{-DP}$ [50]). *Let $f : \mathcal{D} \rightarrow \mathcal{R}$ be an arbitrary function. If for all of the adjacent datasets¹ $\mathcal{D}, \mathcal{D}'$ and any randomized output $s \subseteq \mathcal{R}$, the function f satisfies:*

$$Pr[f(\mathcal{D}) \in s] \leq e^\epsilon Pr[f(\mathcal{D}') \in s] + \delta, \quad (4)$$

where δ is the failure probability.

Then we say that f is (ϵ, δ) -differentially private.

$(\epsilon, \delta)\text{-DP}$ ensures that for all adjacent $\mathcal{D}, \mathcal{D}'$, the privacy loss will be bounded by ϵ with probability at least $1 - \delta$. If $\delta = 0$, we say that f is ϵ -differentially private.

The essence of the noise injection mechanism lies in incorporating noise sourced from a predefined distribution, thereby aligning the data distribution with DP specifications. This strategy aids in obscuring discrepancies between neighboring datasets and fortifying the processed dataset against potential privacy breaches. A commonly adopted method involves injecting Gaussian noise, which provides a more relaxed form of DP protection, as proven by Theorem 1 [51].

Theorem 1. *Let $\epsilon \in (0, 1)$ and δ be arbitrary. For $c^2 \geq 2\ln(\frac{1.25}{\delta})$, the Gaussian Mechanism $n \sim \mathcal{N}(0, \sigma^2)$ with parameter $\sigma \geq \frac{c\Delta f}{\epsilon}$ is (ϵ, δ) -differentially private [51]. The sensitivity Δf is defined as*

$$\Delta f = \max_{x, x'} ||f(x) - f(x')||, \quad (5)$$

where x, x' are the arbitrary adjacent inputs.

¹Two datasets \mathcal{D} and \mathcal{D}' are considered adjacent if they differ by only one sample. Conventionally, adjacent datasets \mathcal{D}' can be derived by either deleting or replicating a single instance from the original dataset \mathcal{D} . For a dataset \mathcal{D} consisting of n instances, there exist precisely $2n$ distinct adjacent datasets.

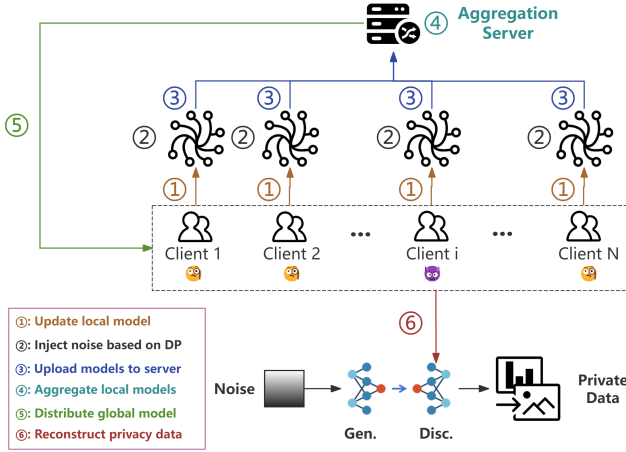


Fig. 1. An FL model with an honest-but-curious client trying to infer private information from the global model. “Gen.” and “Disc.” denote Generator and Discriminator, respectively.

IV. THREAT MODEL

We consider a general FL system consisting of a central aggregation server and a collection of distributed clients, as shown in Figure 1. Below, we discuss the security assumptions and threats for both the server and the individual clients.

- **Aggregation Server.** We assume that the central aggregation server is fully trusted, adhering to its designated role in the FL system. Specifically, we assume that the server faithfully performs the tasks of aggregating model parameters (Step ④ in Figure 1) and distributing correct and complete models without attempting to compromise user privacy or maliciously altering model parameters (Step ⑤ in Figure 1). Addressing malicious server scenarios is out of the scope of this paper.
- **Non-malicious Clients.** We consider most of the clients participating in the FL system to be non-malicious, such as Client 1 and Client N in Figure 1. These clients use local datasets to train models (Step ① in Figure 1) and then upload model parameters to the server (Step ③ in Figure 1), awaiting subsequent global updates.
- **Honest-but-Curious (HBC) Clients.** We assume that there exist HBC clients (e.g., Client i in Figure 1) in the FL system who faithfully execute their designated tasks and upload accurate model parameters. However, these clients exhibit curiosity and seek to reconstruct the private data of other participants. In this paper, we follow related work [9] and assume that HBC clients employ a Generative Adversarial Network (GAN) to reconstruct the sensitive information of fellow clients (Step ⑥ in Figure 1). The discriminator architecture of this GAN aligns entirely with the global model, while the generator architecture adopts a deconvolutional neural network.

V. METHODOLOGY

In this section, we first present an overview of LaDP-FL, followed by a more detailed description of its design modules.

Algorithm 1 The workflow of LaDP-FL on the server side.

Require: Global model w_g^t ; Global training round T ; Server storage collection \mathcal{S} .
Ensure: A protected model \tilde{w}_i^t .

- 1: Initialize the global model w_g^0 and global round $t \leftarrow 0$;
- 2: Distribute the global model w_g^0 ;
- 3: **while** Global round $t \leq T$ **do**
- 4: Randomly activate a subset of \mathcal{C} , denote as \mathcal{AC} ;
- 5: Wait for all the clients in \mathcal{AC} upload their protected model w_i^t by Algorithm 2;
- 6: /* Aggregate the global model */
 $w_g^t = \sum_{w_i^t \in \mathcal{S}} \frac{|\mathcal{D}_i|}{D} w_i^t$;
- 7: Distribute new model w_g^t to all clients.
- 8: $t \leftarrow t + 1$;
- 9: **end while**

Algorithm 2 The workflow of LaDP-FL on the client side at global training round t .

Require: New global model w_g^{t-1} ; Local dataset \mathcal{D}_i ; Local training epoch E ; Learning rate η ; Privacy parameters ϵ, δ, c_i ; Privacy estimation bound B ; Gradients clip bound G_c ; Layer selection parameters R .
Ensure: A protected model \tilde{w}_i^t .

- 1: /* Update local model by new global model */
 $w_{i,0}^t \leftarrow w_g^{t-1}$;
- 2: Initialize $e = 0$;
- 3: **while** local epoch $e \leq E$ **do**
- 4: Compute the loss $\nabla F(w_{i,e-1}^t)$ by local dataset \mathcal{D}_i ;
- 5: /* Clip the local gradients */
 $\nabla F(w_{i,e-1}^t) \leftarrow \frac{\nabla F(w_{i,e-1}^t; \mathcal{D}_i)}{\max(1, \frac{||\nabla F(w_{i,e-1}^t; \mathcal{D}_i)||}{G_c})}$;
- 6: /* Update local models */
 $w_{i,e}^t \leftarrow w_{i,e-1}^t - \eta \nabla F(w_{i,e-1}^t)$;
- 7: $e \leftarrow e + 1$;
- 8: **end while**
- 9: /* Finish local training */
 $w_i^t \leftarrow w_{i,E}^t$;
- 10: /* Estimate the function sensitivity */
 $\Delta f_i = 2\eta E G_c$;
- 11: **for** all layers j in the network w_i^t **do**
- 12: **if** Layer selection: $||w_{i,j}^t|| \geq R$ **then**
- 13: /* Privacy Estimation by Algorithm 3 */
 $P_{i,j} \leftarrow \text{PRIVACY_ESTIMATION}(w_{i,j}^t, w_g^t)$;
- 14: /* Adaptive Noise Injection by Algorithm 4 */
 $\tilde{w}_{i,j}^t \leftarrow \text{NOISE_INJECTION}(w_{i,j}^t, \epsilon, \Delta f_{i,j}, c_i, P_{i,j})$;
- 15: **end if**
- 16: **end for**
- 17: Upload local model \tilde{w}_i^t .

A. System Overview

The workflow of LaDP-FL on both the server side and the client side is illustrated in Algorithms 1 and 2, respectively. Specifically, in Algorithm 1, the server first initializes the federated settings and distributes the initial model to all clients (Lines 1-2). Then, during each global training round, the server randomly selects a subset of activated clients to train the model using their local datasets and awaits their updates (Lines 4-5). Finally, the server aggregates the updates to form a new global model, distributes this new model to all clients, and proceeds to the next global round (Lines 6-8). In Algorithm 2, upon receiving the initial model from the server (Line 1), each activated local client first executes local training (Lines 2-9). Then, the client estimates the sensitivity of the current epoch (Line 10), and iterates through each neural network layer to determine whether it contains essential information for model updates (Lines 11-12). If the norm value of the weights in a certain neural network layer exceeds a predefined

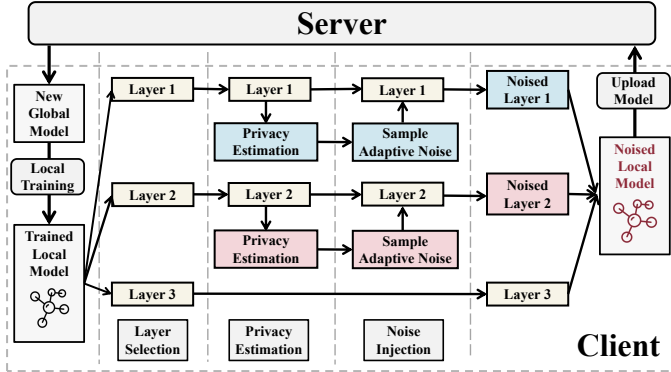


Fig. 2. A visual representation of each module of LaDP-FL. The blue and red squares represent different levels of privacy information associated with different layers, resulting in different amounts of noise injection.

threshold R , the client estimates the privacy level $P_{i,j}$ for that layer, and then enforces an upper bound on $P_{i,j}$ to guarantee fundamental privacy protection (Line 13). Next, based on the derived privacy levels, the client determines the noise range and samples noise to inject into each layer (Line 14). Finally, after processing all neural network layers, the client uploads the noisy model to the server (Line 19).

To better balance privacy protection and model accuracy, LaDP-FL ignores those layers with smaller weights when injecting noise (Line 12 in Algorithm 2). Since pruning away small-weighted layers will not significantly impair the model's predictive ability [23], [25], these smaller weights indicate weaker predictive power. Therefore, LaDP-FL can mitigate the adverse effects of noise on the model's utility while ensuring that privacy is not unduly compromised. For other layers, LaDP-FL first assesses their private content using the KL divergence (Lines 13-14 in Algorithm 2). For layers containing more private information, LaDP-FL will prioritize privacy protection by sacrificing some model utility; otherwise, LaDP-FL will minimize noise injection to enhance model utility (Lines 15-16 in Algorithm 2).

B. System Design

LaDP-FL consists of three modules: layer selection, privacy estimation, and noise injection, as illustrated in Figure 2. We explain each of these modules in more detail below.

1) *Layer Selection*: In this module, LaDP-FL identifies the neural network layers that have a more substantial impact on the predictive performance of the global model. Specifically, upon receiving the latest global model from the server, the client C_i first updates its current local model $w_{i,0}^t$ by replacing it with the previous round's global model w_g^{t-1} . Then, the client employs its local optimizer to update the model for E epochs iteratively and gets a new model $w_{i,E}^t$. Inspired by related work [47], we clip the model's gradients by G_c based on Assumption 1, which ensures the convergence stability of the model during local training.

Assumption 1 (Client-level Bounded Gradients [52], [53]). For $\forall C_i \in \mathcal{C}$, we assume that there exists a constant $G_c \geq 0$

such that its gradient $\nabla F(w_i^t)$ satisfies:

$$\|\nabla F(w_i^t)\| \leq G_c. \quad (6)$$

After completing local training, participants inspect each layer of the neural network to identify those containing significant information. Researchers have employed ablative experiments [54], [55] by removing or replacing specific layers to observe changes in model performance. However, utilizing this strategy to select layers is practically infeasible. This is because conducting control experiments for every neural network layer during the FL process could incur enormous time and resource costs. To address this challenge, LaDP-FL leverages a key insight commonly used for model pruning and compression: *layers with larger weights contribute more significantly to the model's prediction* [23], [25]. Therefore, by calculating the \mathcal{L}_2 norm of each layer and considering those exceeding a threshold R as crucial for maintaining model predictability, LaDP-FL mitigates the impact of noise on the global model. Besides having a significant impact on the model's prediction, these crucial layers also carry important private information. Intuitively, for layers with smaller weights, it is difficult for adversaries to extract useful information from these layers to launch attacks, such as model inversion [9], [56] and membership inference [11], [57], [58]. Hence, LaDP-FL relies on crucial layers for adaptive noise injection, which ensures privacy protection.

2) *Privacy Estimation*: Traditional privacy attacks [9], [11], [56] rely on an aggregated global model to infer private information. Existing DP-FL approaches [18], [20], [48] typically inject uniform noise across all model layers, ignoring the varying risks of different layers to privacy leakage. This one-size-fits-all strategy leads to either excessive utility loss (when over-protecting insensitive layers) or insufficient privacy guarantees (when under-protecting critical layers).

To address this problem, we employ KL divergence for layer-wise privacy estimation based on three fundamental principles:

- 1) **DP as Distribution Alignment**: Differential privacy fundamentally requires neighboring datasets to produce statistically similar outputs [51]. The KL divergence directly measures this similarity through the relative entropy between distributions:

$$KL(p||q) = \mathbb{E}_p \left[\log \frac{p(x)}{q(x)} \right] \quad (7)$$

- 2) **Information-Theoretic Interpretation**: The KL value $KL(w_{i,j}^t||w_{g,j}^t)$ quantifies the minimum additional information (in nats) needed to encode layer j 's weights using the global distribution rather than the local one. This aligns with privacy leakage metrics in [59].
- 3) **Attack Surface Correlation**: As demonstrated in [60], reconstruction attack success probability grows exponentially with decreasing KL divergence between victim and attacker models.

Below, we consider two scenarios for intuitive interpretation:

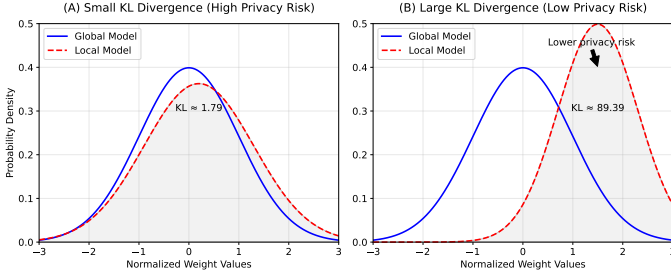


Fig. 3. Illustration of KL divergence's relationship with privacy risk. (A) When $KL \approx 0$, the global model has a higher privacy risk because it closely resembles the local model. (B) When $KL \gg 0$, the local layer reveals little about the global mode due to the significant deviation.

Algorithm 3 The process of privacy estimation.

Require: The parameter matrix of the j -th layer within the local model w_i^t , denoted as $w_{i,j}^t$; Global model w_g^t .
Ensure: The quantified privacy of the j -th layer $P_{i,j}$.

- 1: Extract the parameter matrix of the j -th layer within the global model, denoted as $w_{g,j}^t$;
- 2: Flatten the parameter matrices $w_{i,j}^t$ and $w_{g,j}^t$;
 ▷ i.e., flatten to 1-D vectors, such as from $\mathbb{R}^{m \times n}$ to \mathbb{R}^{mn} .
- 3: Normalize the layers using $softmax()$;
 ▷ e.g., $[1, 2, 3] \rightarrow [0.09, 0.24, 0.67]$
- 4: Calculate $P_{i,j}$ based on the KL divergence using Equation 8;
 ▷ e.g., using function $kl_div()$ in the package `torch.nn.functional`.
- 5: Clip $P_{i,j}$ by the boundary B .
 $P_{i,j} \leftarrow \min(P_{i,j}, B)$.

- **Small KL divergence:** Layer weights closely match the global distribution → Higher privacy risk (requires more noise)
- **Large KL divergence:** Significant deviation from global distribution → Lower privacy risk (needs less protection)

Algorithm 3 shows the detailed procedure for privacy calculation. LaDP-FL first extracts the parameter matrix $w_{g,j}^t$ of the j -th layer within the global model (Line 1). Then, LaDP-FL flattens and normalizes the selected layers (Lines 2 and 3) to ensure the non-negativity of the KL divergence. Finally, LaDP-FL computes $P_{i,j}$ using Equation 8 (Line 4) and clips it to an upper bound B . (Line 5) A large $P_{i,j}$ suggests that the weight distribution in the j -th layer of the local model exhibits a substantial deviation compared to its counterpart in the global model, thereby better safeguarding privacy. This is because the substantial deviation makes it difficult for HBC participants to recover information about the j -th layer of the victim model from the global model. Hence, LaDP-FL leverages $P_{i,j}$ to adjust the noise injection amount adaptively. In particular, as $P_{i,j}$ increases, LaDP-FL reduces the noise injection amount (i.e., $\sigma_{i,j} \propto 1/P_{i,j}$) to the corresponding layers to protect privacy. LaDP-FL also controls the boundary of $P_{i,j}$ to prevent situations where the noise injection amount is too small and tends to zero (see Section V-B3).

Definition 2 (Layer Privacy Metric). *For layer j in client i 's model w_i^t , the privacy content $P_{i,j}$ is:*

$$P_{i,j} = \min(KL(w_{i,j}^t || w_{g,j}^t), B), \quad (8)$$

where B is a clipping boundary ensuring minimum noise injection.

Algorithm 4 Layer-wise Adaptive Noise Injection

Require: Layer parameters $w_{i,j}^t \in \mathbb{R}^{m_1 \times \dots \times m_d}$, ϵ , $\Delta f_{i,j}$, c_i , $P_{i,j}$.
Ensure: Noisy layer $\tilde{w}_{i,j}^t$.

- 1: Compute $\sigma_{i,j} = \frac{c_i \Delta f_{i,j}}{\epsilon P_{i,j}}$
- 2: Generate noise matrix $n_{i,j}$ where:

$$n_{i,j}^{(k_1, \dots, k_d)} \sim \mathcal{N}(0, \sigma_{i,j}^2) \quad \forall k_l \in 1, \dots, m_l$$
- 3: Element-wise addition: $\tilde{w}_{i,j}^t = w_{i,j}^t + n_{i,j}$

This approach provides three key advantages: (1) **Data-Agnostic**: Requires no knowledge of other clients' data distributions. (2) **Layer-Adaptive**: Captures varying sensitivity across network depths. (3) **Attack-Resistant**: Directly correlates with reconstruction difficulty (verified in Section VII-C).

3) *Noise Injection:* The noise injection process critically impacts both privacy protection and model utility in FL systems. Excessive noise degrades model accuracy and training stability, while insufficient noise compromises privacy. To address these challenges, LaDP-FL implements an adaptive layer-wise noise injection mechanism with three key innovations: (1) privacy-aware noise scaling, (2) dimensional consistency enforcement, and (3) cross-client compatibility.

First, we conduct a layer-wise sensitivity analysis and derive layer-specific sensitivity bounds, taking into account the non-IID data distribution across clients, based on Theorem 2.

Theorem 2. *For client C_i with local gradient $\nabla F(w_i^t)$ clipped by G_c , the sensitivity of layer $w_{i,j}$ satisfies:*

$$\Delta f_{i,j} \leq 2\eta E G. \quad (9)$$

where η is the learning rate and E is local epochs.

This elucidates how to estimate the sensitivity in Theorem 1, thereby determining the noise variance by the Gaussian mechanism (proof sketch in Supplemental Material).

Algorithm 4 details our dimensional-consistent noise injection process. It includes two key implementation aspects: (1) **Dimensional Matching**: For different selected layers (e.g., convolutional layer with $64 \times 64 \times 3 \times 3$ dimensions in ResNet-18), we generate noise tensors matching the parameter dimensions exactly. (2) **Cross-client Consistency**: All clients within the same FL select layers from the same model architecture, thus ensuring that all distributed clients generate identically shaped additive noise tensors for the same selected layers.

LaDP-FL adopts an adaptive noise scaling strategy, where the standard deviation of the noise follows:

$$\sigma_{i,j} = \frac{c_i \Delta f_{i,j}}{\epsilon P_{i,j}}, \quad (10)$$

where $P_{i,j}$ is the clipped KL-divergence privacy estimate. This creates an inverse relationship where:

- Low $P_{i,j}$ (similar layers) ⇒ Larger noise (stronger privacy)
- High $P_{i,j}$ (dissimilar layers) ⇒ Smaller noise (preserves useful information)

LaDP-FL ensure robust performance under non-IID data distribution because of two mechanisms: (1) **Privacy Thresholding**: A minimum noise level B prevents under-protection.

(2) **Dynamic Privacy Estimation:** Models exhibit variations in layer weights across different data distributions; dynamic privacy estimation mechanisms capture these variations and adaptively regulate noise injection to maintain data privacy and model utility concurrently. As demonstrated in Section VII-B6, LaDP-FL achieves an average of 25.21% accuracy improvement over all baselines in extreme non-IID settings.

VI. THEORETICAL ANALYSIS

In this section, we conduct a theoretical analysis of the privacy guarantees offered by LaDP-FL. We further conduct the convergence analysis of LaDP-FL in scenarios involving restricted gradients and noises, demonstrating that LaDP-FL has the capability to converge toward the optimal solution.

A. Privacy Analysis

Based on Theorem 1, we have established that under standard Gaussian mechanisms, (ϵ, δ) -DP is satisfied when the variance satisfies $\sigma \geq \frac{c\Delta f}{\epsilon}$, where $c^2 > 2 \ln \frac{1.25}{\delta}$. To provide the theoretical privacy guarantees, we first present the following theorem:

Theorem 3. *Given privacy budget ϵ , failure probability δ and the KL-privacy estimation bound B , if the parameter c_i for the client \mathcal{C}_i satisfies:*

$$c_i \geq \begin{cases} \frac{(\sqrt{\ln \frac{2}{\pi \delta^2}} + \sqrt{\ln \frac{2}{\pi \delta^2} + 8\epsilon})B}{4}, & \text{if } 0 < \delta \leq \sqrt{\frac{2}{\pi e^4}} \\ \frac{(1 + \sqrt{1 + 2\epsilon})B}{2}, & \text{if } \sqrt{\frac{2}{\pi e^4}} < \delta < 1. \end{cases} \quad (11)$$

Then, our proposed system LaDP-FL satisfies (ϵ, δ) -DP if the client \mathcal{C}_i adds Gaussian noise with variance in Equation 10.

Proof. See Section XI in the Supplemental Material. \square

Theorem 3 ensures that each round of noise injection satisfies (ϵ, δ) -DP guarantees. In the entire FL training process, each client requiring privacy protection injects noise into their updates according to Theorem 3's constraints and then uploads these updates to the server. Therefore, the entire training process can theoretically guarantee DP protection.

B. Convergence Analysis

First, we introduce some assumptions, standard in the federated learning literature, for our convergence analysis.

Assumption 2 (L-Smoothness [3]). *Objective function $F(x)$ satisfies L-Lipschitz Smoothness, which means that for $\forall x, y$,*

$$F(y) - F(x) \leq \nabla F(x)^T (y - x) + \frac{L}{2} \|y - x\|^2, \quad (12)$$

where $L > 0$ is a constant.

Assumption 3 (μ -Polyak-Lojasiewicz condition [61]). *Objective function $F(x)$ satisfies μ -Polyak-Lojasiewicz condition, i.e., for $\forall x$,*

$$F(x) - F^* \leq \frac{1}{2\mu} \|\nabla F(x)\|^2, \quad (13)$$

where $\mu > L$ is a constant and F^* is the global optima of $F(x)$.

Assumption 4 (Bounded Noise). *To guarantee the effectiveness of the training, we assume that the amount of noise $n_{i,j}$ added to each layer of a J -layer neural network is bounded by $N_c > 0$, denoted by:*

$$\|n_{i,j}\| \leq N_c. \quad (14)$$

Given the bounded noise, the following corollary holds:

Corollary 1. *If the global model has J layers, the additional noise n_i^t in global round t satisfies:*

$$\|n_i^t\| = \left\| \sum_{j=1}^J n_{i,j}^t \right\| \leq J N_c, \quad (15)$$

where $n_{i,j} \sim N(0, \sigma_{i,j}^2)$ in LaDP-FL, $\sigma_{i,j}$ is defined in Equation 10 and satisfying the constraint condition in Equation 11.

Subsequently, leveraging the bounded noise assumption, we derive a theorem to establish the convergence of LaDP-FL under (ϵ, δ) -privacy constraints.

Theorem 4 (Convergence of LaDP-FL). *Assume that Assumptions 1-4 hold and let L, μ, G_c, N_c be defined therein. For a J -layer network, let the learning rate η satisfy $\frac{2JN_c}{G_c} > \eta > \frac{2JN_c}{G_c} - \frac{\mu - L}{LG_c \mu}$, then we have the following convergence results:*

$$\begin{aligned} \mathbb{E}[F(w_g^t)] - F^* &\leq \left(\frac{L + \psi \mu L}{\mu} \right)^t (\mathbb{E}[F(w_g^0)] - F^*) \\ &\quad + \frac{\psi + 2\phi}{2} \sum_{n=0}^{t-1} \left(\frac{L + \psi \mu L}{\mu} \right)^n, \end{aligned} \quad (16)$$

where $0 < \frac{L + \psi \mu L}{\mu} < 1$, $\phi = \frac{L\eta^2}{2} G_c^2 + 2LJ^2 N_c^2$, and $\psi = 2JN_c - \eta G_c$.

Proof. See Section XII in the Supplemental Material. \square

Theorem 4 demonstrates that although LaDP-FL injects random noise into the training process to ensure privacy protection for local clients' updates, this injection does not compromise the model's convergence performance when the noise size is limited. That said, LaDP-FL preserves the convergence process, thereby guaranteeing the effectiveness of the entire FL training.

VII. EXPERIMENTAL RESULTS

In this section, we first describe our evaluation setup, including the FL framework, the client configurations, the datasets and models, and the attack settings. To evaluate LaDP-FL, we focus on answering the following research questions:

RQ 1: How is LaDP-FL's performance in terms of privacy budget, prediction accuracy, noise injection amount, and resource consumption?

RQ 2: Can LaDP-FL defend against real-world adversarial attacks?

RQ 3: How sensitive is LaDP-FL to privacy assessment?

All experiments were conducted using an Intel(R) Xeon(R) CPU E5-2620 v4 @ 2.20GHz processor and an NVIDIA

GeForce GTX 1080 Ti graphics card. Only representative results are included in this paper.

A. Experimental Setup

FEDERATED LEARNING FRAMEWORK. We implement LaDP-FL on a synchronous FL system with 100 clients and one central server, simulating real-world deployment scenarios. The system architecture follows the threat model in Section IV, with one Honest-but-Curious (HBC) client among non-malicious participants.

DATA DISTRIBUTION. We evaluate under realistic non-IID conditions using *Private Label Isolation*, where one target class (e.g., “dog” in CIFAR-10) is excluded from the HBC client to simulate sensitive data protection scenarios.

TRAINING CONFIGURATION. All experiments use:

- 400 global rounds with 10% client activation per round.
- Local training: $E = 2$ epochs, batch size = 50, $\eta = 0.1$.
- Differential privacy: $\delta = 0.02$ (reciprocal of batch size).
- Gradient clipping: $G_c = 20$ (validated in Section VII-B2).

DATASETS & MODELS. We conduct comprehensive evaluations using the following dataset-model combinations.

TABLE I
DATASET-MODEL COMBINATIONS

Evaluation	Dataset	Classes	Model(s)
Performance	CIFAR-100	100	ResNet-18, CNN
	CIFAR-10	10	ResNet-18, CNN
Attack defense	CIFAR-10	10	ResNet-18
	FEMNIST	62	CNN

ATTACK SIMULATION. We evaluate against state-of-the-art reconstruction attacks using:

- ACGAN [62] with discriminator architecture matching the global model.
- Fréchet Inception Distance (FID) scores as a reconstruction quality metric (Detailed results are provided in Supplemental Material).

B. Performance Evaluation (RQ 1)

We conduct comprehensive experiments to evaluate LaDP-FL’s effectiveness across five dimensions: (1) privacy budget impact, (2) model accuracy, (3) noise efficiency, (4) computational overhead, and (5) data heterogeneity impact. Our evaluation compares LaDP-FL against six baselines: vanilla FL (no DP) [1], Full DP [31], Time-Varying DP [18], Sensitive DP [17], DPA LDP [32], and AdapLDP [33]. All experiments follow the setup in Section VII-A.

1) Impact of Privacy Budget: Figure 4 demonstrates LaDP-FL’s robustness across varying privacy budgets ($\epsilon \in [0.16, 0.4]$) on ResNet-18. We highlight two key findings: (1)

Accuracy Preservation: At $\epsilon = 0.16$, LaDP-FL maintains 22.4% accuracy on CIFAR-100 vs. 12.23% for Full DP (83.15% improvement). As ϵ increases to 0.4, this gap narrows to 9.62% (61.67% vs. 52.05%). (2) **Graceful Degradation:** When reducing ϵ from 0.4 to 0.16, LaDP-FL exhibits an

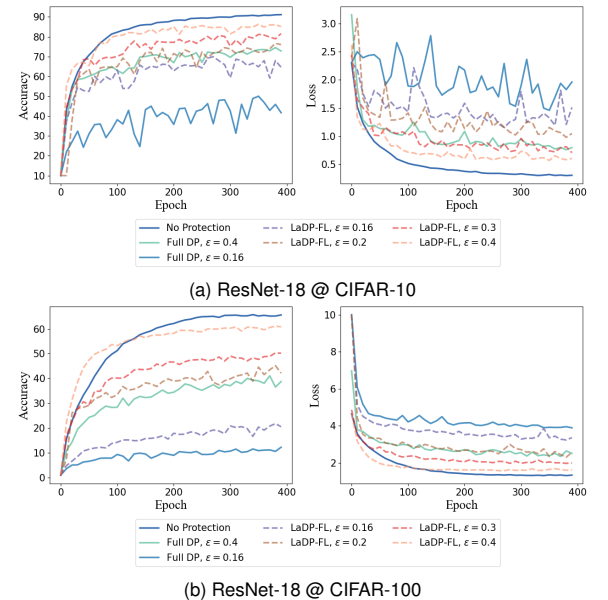


Fig. 4. The influence of the privacy budget ϵ on global accuracy and loss when using ResNet-18 on different datasets.

TABLE II
ACCURACY PERFORMANCE OF LADP-FL AND BASELINES.

Scenarios	Method	ResNet-18@CIFAR-10					
		LaDP-FL (Ours)	Full DP	Time-Varying DP	Sensitive DP	DPA LDP	AdapLDP
Acc. (%)	0.2	77.82	58.35	63.65	64.43	66.54	73.90
	0.3	82.29	58.58	62.54	67.64	73.77	77.12
	0.4	87.12	60.71	66.79	69.68	77.94	83.28
	0.5	90.06	70.59	78.51	84.68	79.36	88.39
Average Improvement Rate		-	36.22%	24.73%	18.45%	13.44%	4.62%
Scenarios							
Acc. (%)	0.2	15.69	1.23	1.87	2.87	7.73	12.04
	0.3	18.56	1.52	2.03	3.55	12.56	16.88
	0.4	39.45	10.83	22.44	25.12	33.14	37.29
	0.5	40.38	22.13	28.93	35.57	35.11	39.26
Average Improvement Rate		-	660.85%	417.18%	235.02%	46.20%	12.23%

average accuracy drop of 18.41% (vs. 39.88% for Full DP) across CIFAR-10/100 datasets, indicating more stable performance. This stability stems from LaDP-FL’s layer-adaptive noise injection, which strategically prioritizes preserving critical model parameters.

2) Accuracy Comparison: Table II shows the experimental results of LaDP-FL’s prediction accuracy compared to SOTA DP mechanisms under identical privacy budgets ($\epsilon \in [0.2, 0.5]$). We highlight three key findings: (1) **Low-Budget Superiority:** At $\epsilon = 0.2$, LaDP-FL improves accuracy by 33.37% over Full DP when training ResNet-18 on CIFAR-10, outperforming Time-Varying DP (22.26%) and Sensitive DP (20.78%). The advantage is more pronounced when training CNN on CIFAR-100 with 498.93% average improvement. (2) **High-Budget Convergence:** When $\epsilon = 0.5$, LaDP-FL approaches non-DP performance on CIFAR-10, while other methods show significant gaps (up to 20.14% degradation). (3) **Consistent Gains:** Across all scenarios, LaDP-FL achieves average improvements of: 236.32% over Full DP, 144.93% over Time-Varying DP, 102.42% over Sensitive DP, 25.18% over DPA LDP, and 6.1% over AdapLDP.

TABLE III
NOISE SCALE PERFORMANCE OF LADP-FL AND BASELINES.

Method	LaDP-FL (Ours)	Full DP	Time- Varying DP	Sensitive DP	DPA LDP	AdapLDP
Scenarios						
		ResNet-18@CIFAR-10				
Noise Scale ϵ	0.2	275,447	727,901	862,998	242,583	386,453
	0.3	132,365	505,266	295,231	165,234	261,698
	0.4	87,563	383,945	224,129	95,468	241,778
	0.5	51,658	203,968	193,487	53,997	156,947
Average Reduction Rate	-	71.96%	64.37%	4.74%	52.25%	72.80%
Scenarios						
		CNN@CIFAR-100				
Noise Scale ϵ	0.2	22,968	77,523	50,803	23,854	35,603
	0.3	19,297	52,652	34,114	21,271	37,329
	0.4	9,028	42,236	23,578	9,548	27,668
	0.5	8,677	25,786	18,270	8,933	10,119
Average Reduction Rate	-	69.68%	53.11%	5.33%	41.35%	66.85%

TECHNICAL INSIGHT. Existing approaches treat neural networks monolithically, while LaDP-FL carefully identifies and assesses the privacy capabilities of neural network layers that contribute more significantly to the final model’s prediction ability. This prevents excessive noise injection into layers that do not compromise privacy but provide stronger predictive ability. Complete results and statistical significance tests are provided in Section XIV in the Supplemental Material.

PRIVACY-UTILITY TRADEOFF. Overall, LaDP-FL achieves SOTA privacy-utility tradeoffs, offering stronger privacy guarantees while maintaining superior utility. In empirical evaluations on CIFAR-10 with ResNet-18, LaDP-FL outperforms Full-DP by reducing injected noise by 71.96% and improving model accuracy by 36.23%. Compared to Time-Varying DP and Sensitive DP, it reduces noise injection by 80.3% and 9.4% across all scenarios, respectively, while improving accuracy by 21.4% and 15.9%. Under identical privacy budgets, on average, LaDP-FL surpasses DPA LDP and AdapLDP with 25.18% and 6.1% higher accuracy, respectively, and reduces noise volume by 40.54% and 68.31%.

From a privacy perspective, LaDP-FL significantly curtails cumulative privacy budget consumption during training, achieving reductions of 63.3% (vs. Full-DP), 76.7% (vs. Time-Varying DP), 26.6% (vs. Sensitive DP), 71.6% (vs. DPA LDP), and 63.3% (vs. AdapLDP). These results demonstrate that LaDP-FL: (1) optimizes noise injection via fine-grained calibration, minimizing utility degradation; and (2) rigorously controls privacy budget expenditure, enhancing end-to-end protection guarantees—a critical advancement for differentially private ML in practice.

3) *Noise Scale Comparison:* We quantify noise using the \mathcal{L}_2 norm, the de facto standard for perturbation measurement in adversarial learning [63], [64]. For each privacy mechanism, we compute the cumulative noise injected over 400 global training rounds. Table III summarizes the results.

KEY FINDINGS. For ResNet-18/CIFAR-10 at $\epsilon = 0.5$, LaDP-FL reduces noise by 74.67% compared to Full DP [31], outperforming Time-Varying DP (5.14% reduction) and Sensitive DP (73.53% reduction). DPA LDP achieves a 23.05% average reduction, while AdapLDP matches Full DP’s noise volume. At stricter privacy ($\epsilon = 0.2$), LaDP-FL maintains an average 41.59% reduction while achieving higher accuracy than base-

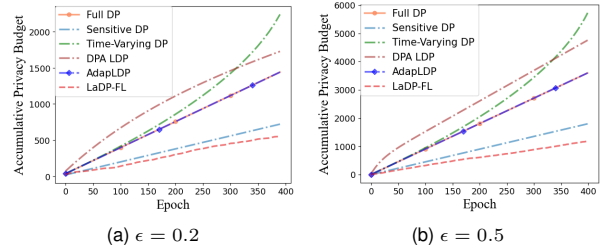


Fig. 5. The comparison of accumulative privacy budget under different privacy budgets ϵ between LaDP-FL and baselines when training ResNet-18 on the CIFAR-10 dataset. Notably, the curves for Full DP and AdapLDP completely overlap; we distinguish them using distinct markers at varying intervals.

lines, demonstrating superior privacy-utility tradeoffs.

We evaluate LaDP-FL against all DP variants, averaging results across all scenarios (see Section XIV in the Supplemental Material for methodology). Compared to: (1) Full DP/AdapLDP: 69.32%/68.31% reduction, (2) Time-Varying DP: 51.35% reduction, (3) Sensitive DP: 1.2% reduction (marginal), and (4) DPA LDP: 40.54% reduction. Overall, LaDP-FL achieves a 46.14% average noise reduction versus all SOTA methods.

TECHNICAL INSIGHT. Full DP and AdapLDP inject static noise, while Time-Varying DP and DPA LDP use exponential decay to reduce final noise. Sensitive DP adjusts noise per iteration via sensitivity estimation. Conversely, LaDP-FL adopts a layer-aware approach: (1) Dynamic per-layer allocation: Noise scales with layer-specific requirements. (2) Client selection variance: Fluctuations arise from differing per-round client contributions, proving adaptability to evolving privacy needs.

4) *Accumulative Privacy Budget Comparison:* To rigorously quantify the privacy-utility trade-off, we evaluate the cumulative privacy budgets of LaDP-FL and baselines by Naive Composition Theorem [51] (detailed derivations in Section XIII of the Supplemental Material). Figure 5 presents the results when training ResNet-18 on CIFAR-10 ($\delta = 0.02$).

KEY FINDINGS. Full DP demonstrates linear budget growth with training rounds (e.g., slope=3.6 when training ResNet-18 under $\epsilon = 0.2$), as expected from fixed-noise injection. Time-Varying DP and DPA LDP exhibit 57.3% and 26.04% higher cumulative ϵ than Full DP, respectively, confirming their privacy relaxations for utility gains. AdapLDP maintains an identical ϵ progression to Full DP, as both employ equivalent noise mechanisms. Sensitive DP reduces ϵ accumulation by 51.2%, demonstrating its adaptive protection approach.

LaDP-FL achieves 63.3% lower ϵ accumulation than Full DP through our *layer-wise selective injection* and *adaptive variance scaling* strategies. Crucially, this improvement is attained while maintaining model utility, as LaDP-FL’s noise allocation is optimized via our proposed privacy-aware distribution mechanism. The results are statistically significant ($p = 2.64e-5$ under Mann-Whitney U Test) and consistent across all four experimental scenarios (Section XIV in the Supplemental Material).

SECURITY IMPLICATIONS. The reduced ϵ accumulation of LaDP-FL indicates a stronger capability of privacy preservation. Notably, although LaDP-FL decreases the amount

TABLE IV
RESOURCE UTILIZATION OF LADP-FL AND BASELINES.

Method	LaDP-FL (Ours)	Full DP	Time-Varying DP	Sensitive DP	DPA LDP	AdapLDP	
Scenario							
ResNet-18@CIFAR-10							
Training Duration (s)	0.2	93,775	80,110	86,423	83,793	91,687	94,773
	0.3	93,455	82,157	83,151	86,363	89,569	92,042
	0.4	94,985	81,511	87,562	82,443	90,524	96,111
	0.5	96,008	82,018	89,110	84,008	92,272	95,647
Average Incremental Rate	-	16.10%	9.28%	12.41%	3.90%	-0.08%	
Scenario							
CNN@CIFAR-100							
Training Duration (s)	0.2	16,731	15,120	16,368	16,081	16,441	16,934
	0.3	16,795	15,236	15,831	16,092	16,398	16,765
	0.4	16,963	15,045	15,713	16,045	16,613	16,782
	0.5	16,621	15,013	15,963	16,140	16,286	16,980
Average Incremental Rate	-	11.09%	5.10%	4.28%	2.09%	-0.51%	

of noise injection, it achieves this by adaptively scaling or shrinking the variance for different layers and targeting noise injection at fewer, yet impactful layers.

5) *Resource Comparison*: Our resource evaluation demonstrates two key findings:

KEY FINDINGS. As shown in Table IV, compared to Full DP, LaDP-FL introduces an average of 13.56% additional training time across scenarios. This overhead reduces to 3%-8% when compared to adaptive methods (Time-Varying DP, Sensitive DP, and DPA LDP), and becomes comparable to AdapLDP.

PRACTICAL IMPLICATIONS. The absolute overhead (max +17.06%) translates to <4 additional hours for ResNet-18 training - a reasonable tradeoff for the achieved privacy benefits (Section VII-B2). We note this overhead would diminish proportionally with hardware improvements, as the computational complexity remains within $O(J)$ of baseline methods, where J denotes the depth of the neural network.

6) *Impact of Data Heterogeneity*: Our previous evaluation (Sections VII-B1–VII-B5) used a non-IID distribution (Section VII-A) where non-malicious clients had complete label coverage while only HBC clients lacked the private label. To evaluate LaDP-FL’s resilience to data heterogeneity, we conduct experiments with ResNet-18 on CIFAR-10 under two pathological non-IID distributions: (1) **Distribution I (Label Scarcity)**: 99 non-malicious clients have data with 4 labels (including the private label), while 1 HBC client has 3 labels (excluding the private label). All clients maintain equal data quantities. (2) **Distribution II (Quantity Skew)**: Non-private data follows a Hetero-Dirichlet Distribution [65] ($\alpha = 0.01$) across all clients, while private data follows another Hetero-Dirichlet distribution ($\alpha = 0.01$) among the 99 non-malicious clients. Figure 6 visualizes these distributions by showing data allocations for 4 randomly selected non-malicious clients and 1 HBC client, with Label 10 representing private data.

KEY FINDINGS. (1) **Accuracy Superiority**: LaDP-FL maintains significant accuracy advantages: 38.1% over Full DP, 25.5% over Time-Varying DP (Distribution I), and 80.5% over Full DP, 51.5% over Time-Varying DP (Distribution II). (2) **Noise Efficiency**: Despite distribution skewness, LaDP-FL achieves 3.09% average noise reduction vs. Sensitive DP and minimal noise inflation compared to fixed-schedule baselines.

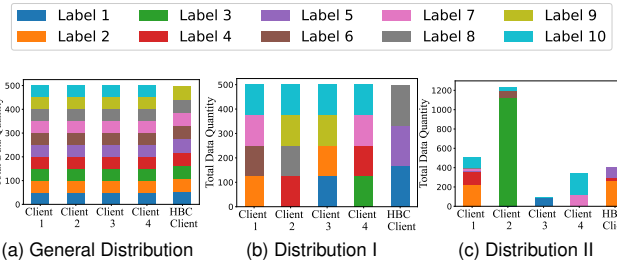


Fig. 6. Data distributions across clients under different heterogeneity settings. Label 10 denotes private data.

TABLE V
PERFORMANCE UNDER EXTREME DATA HETEROGENEITY ($\epsilon \in \{0.2, 0.5\}$).

ϵ	Method	Distribution I		Distribution II	
		Acc. (%)	Noise Scale	Acc. (%)	Noise Scale
-	No Protection	61.33	-	45.16	-
	Full DP	30.32	727,894	15.13	727,895
	Time-Varying DP	34.44	356,555	17.77	356,558
	Sensitive DP	38.76	253,336	21.39	283,316
	DPA LDP	39.07	398,653	24.95	398,153
	LaDP-FL (Ours)	42.13	719,643	19.1	700,645
0.2	Full DP	35.49	203,955	17.33	211,161
	Time-Varying DP	37.88	178,278	20.94	162,628
	Sensitive DP	40.11	87,669	26.03	112,989
	DPA LDP	43.77	150,691	27.91	140,293
	AdapLDP	46.62	197,558	29.52	229,980
	LaDP-FL (Ours)	48.73	84,013	31.79	108,364
0.5	Full DP	35.49	203,955	17.33	211,161
	Time-Varying DP	37.88	178,278	20.94	162,628
	Sensitive DP	40.11	87,669	26.03	112,989
	DPA LDP	43.77	150,691	27.91	140,293
	AdapLDP	46.62	197,558	29.52	229,980
	LaDP-FL (Ours)	48.73	84,013	31.79	108,364

(3) **Robustness**: No failure cases observed in privacy-utility tradeoffs, demonstrating consistent superiority across all tested scenarios.

TECHNICAL INSIGHT. The results stem from LaDP-FL’s dynamic noise adaptation through its Layer Selection and Privacy Estimation Modules, contrasting with the static approaches of Full DP (727,894 noise scale) and Time-Varying DP (356,555 noise scale). While extreme heterogeneity necessitates slight noise increases (251,207 \rightarrow 274,003), LaDP-FL’s adaptive mechanism preserves better utility than sensitivity-based alternatives like Sensitive DP (253,336 \rightarrow 283,316).

C. Defense Performance (RQ 2)

We evaluate LaDP-FL’s defense against targeted class-level reconstruction attacks (Section VII-A), where adversaries aim to recover private-class data (e.g., class ‘5’). Unlike pixel-wise metrics (PSNR/SSIM), we focus on distributional similarity using the Fréchet Inception Distance (FID), which quantifies the Wasserstein-2 distance between real and reconstructed private-class distributions in Inception-v3 feature space.

VISUAL RECONSTRUCTION ANALYSIS. Figure 7 shows the reconstruction results, where black-labeled classes represent public data shared across all clients, and red-labeled classes indicate private data exclusive to victim clients. Among all protection strategies, LaDP-FL provides the strongest protection, as the images reconstructed by the HBC client based on LaDP-FL are the most distorted from their counterparts. LaDP-FL achieves an FID of 121.02 and 83.13 on the privacy data within CIFAR-10 and FEMNIST, respectively (vs. 52.77 and 24.35 for no protection), indicating an average of 17.58% greater protection than Full DP (FID=110.65 and 66.1).

Protection Strategy	CIFAR-10			FEMNIST		
	car	horse	bird	A	e	5
No Protection						
Full DP						
Time-Varying DP						
Sensitive DP						
DPA LDP						
AdapLDP						
LaDP-FL (Ours)						

Fig. 7. The defensive capabilities of different privacy defense strategies against private data reconstruction attacks, where the black label indicates the class data shared by all clients and the red label indicates the private data only possessed by the victim clients.

D. Necessity of Privacy Estimation (RQ 3)

To rigorously evaluate the impact of KL-divergence-based privacy estimation in LaDP-FL, we conduct a controlled ablation study comparing two variants: (1) LaDP-FL with privacy estimation enabled and (2) LaDP-FL with privacy estimation disabled. We measure their performance across two key metrics: model utility (test accuracy) and noise injection dynamics, as illustrated in Figure 8.

KEY FINDINGS. (1) **Utility Preservation:** Disabling privacy estimation degrades model accuracy by 15.97% (high noise, $\epsilon = 0.2$) and 4.74% (low noise, $\epsilon = 0.5$), demonstrating that adaptive noise calibration is critical for balancing privacy-utility trade-offs. (2) **Noise Adaptation:** Without privacy estimation, noise injection remains relatively static across layers and clients. In contrast, LaDP-FL's privacy-aware optimization dynamically tunes noise magnitudes per layer and client, reducing redundancy (e.g., lowering noise in non-sensitive layers) while enforcing stronger protection where needed. This adaptability improves privacy guarantees without sacrificing accuracy.

Our results validate that KL-divergence-based estimation is not merely auxiliary but fundamental to LaDP-FL's design. The module's ability to quantify and react to privacy risks in real time distinguishes it from static DP-FL variants, enabling finer-grained noise allocation.

VIII. DISCUSSION

A. Implementation Complexity and Layer Selection

While selecting critical layers for noise injection introduces additional computations compared to full-model DP approaches, LaDP-FL's complexity remains linear with respect to network depth (i.e., $O(J)$ for J layers). This is identical to the complexity of other DP-based FL approaches, as those algorithms must also iterate through all model layers and generate noise matrices matching each layer's parameter size for perturbation. In contrast, after processing all layers through its layer selection module, LaDP-FL only perturbs a small

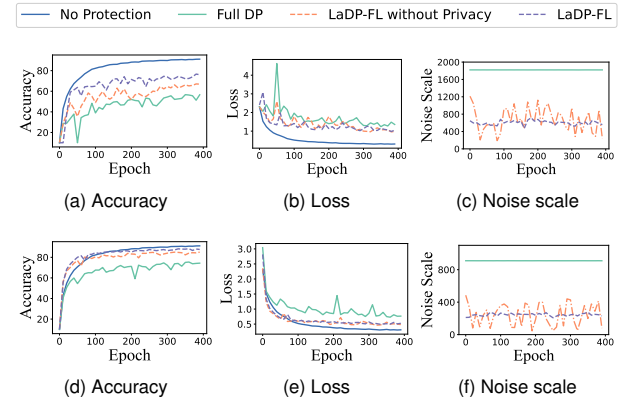


Fig. 8. The impact of privacy assessment component on global accuracy, loss function, and noise injection under $\epsilon = 0.2$ ((a)-(c)) and $\epsilon = 0.5$ ((d)-(f)).

number of selected layers, thereby maintaining this linear complexity. As shown in Table IV, these optimizations result in only 10.23%-17.05% increased computation time compared to Full DP, while providing superior privacy-utility tradeoffs. For very deep networks, our experiments on ResNet-152 (see results in the Supplemental Material) demonstrate that LaDP-FL achieves 53.04% of the accuracy improvement rate while only introducing overhead by 7.27% compared to Full DP.

B. Scalability in Large-Scale Federated Learning

DEEP MODEL SCALABILITY: As discussed in Section VIII-A, LaDP-FL achieves the same complexity, $O(J)$, as other DP-based FL algorithms. When deploying LaDP-FL on large models, all algorithms incur additional computational overhead. While advanced hardware resources (e.g., more powerful GPUs) or optimization algorithms (e.g., LoRA [66]) can mitigate this computational burden, addressing this challenge is beyond the scope of this paper.

MULTI-CLIENT CONSIDERATIONS: The non-IID robustness analysis (Sections V-B3 and VII-B6) confirms LaDP-FL's effectiveness across heterogeneous clients. Meanwhile, LaDP-FL does not require any collaboration between clients, as all operations are performed independently by each client, ensuring scalability with respect to the number of clients.

COMMUNICATION EFFICIENCY: Compared to Full DP (the fundamental DP-based FL algorithm), LaDP-FL requires no additional information transmission during communication, maintaining high efficiency. Furthermore, because LaDP-FL imposes no communication-specific constraints, it remains entirely orthogonal to existing advanced FL communication optimization algorithms [67]–[69] and can be seamlessly integrated with them.

C. KL Divergence and Noise Injection Sensitivity

The KL divergence ($P_{i,j}$) quantifies the information distance between local and global layer distributions, serving as our privacy risk indicator. The noise injection process follows Equation 10. In this equation, when a small change ΔP in $P_{i,j}$ is introduced, we have $\sigma_{i,j} + \Delta\sigma = \frac{c_i \Delta f_{i,j}}{\epsilon(P_{i,j} + \Delta P)}$. By

substituting $\sigma_{i,j}$ from Equation 10 into the equation, we obtain $\Delta\sigma = -\frac{c_i \Delta f_{i,j}}{\epsilon P_{i,j} (P_{i,j}/|\Delta P|+1)}$. Given that $c_i, \Delta f_{i,j}, \epsilon, P_{i,j} \geq 0$, we derive $|\Delta\sigma| = \frac{c_i \Delta f_{i,j}}{\epsilon P_{i,j} (P_{i,j}/|\Delta P|+1)}$.

This design ensures: (1) **Proportional Protection**: noise injection exhibits a reciprocal square relationship with the KL divergence (indicating the level of private information). (2) **Stability**: The reciprocal relationship prevents noise explosion when $P_{i,j} \rightarrow 0$ through our clipping bound B . (3) **Adaptivity**: The $\Delta\sigma/\Delta P$ sensitivity derived above automatically adjusts noise scales during training. As shown in Figure 8, this mechanism reduces unnecessary noise by 69.32% compared to Full DP while maintaining privacy guarantees.

D. Practical Deployment Considerations

LaDP-FL's modular design enables integration with existing FL frameworks like TensorFlow Federated and PySyft, as well as compatibility with common operating systems such as Windows and Ubuntu, facilitating deployment across most device environments. However, it still faces deployment challenges inherent to all FL systems, such as heterogeneous battery resources and unstable network conditions. Notably, our primary objective is to enhance the privacy-utility trade-off in privacy-sensitive scenarios, while addressing these specific deployment limitations falls outside the scope of this work.

IX. CONCLUSION

We present LaDP-FL, the first layer-wise adaptive noise injection framework for FL that achieves an optimal privacy-utility tradeoff. By selectively perturbing critical layers based on their privacy level (measured via KL divergence) and contribution to model utility, LaDP-FL significantly reduces unnecessary noise injection while maintaining strong DP guarantees. Theoretical analysis confirms LaDP-FL's convergence and asymptotic optimality under standard assumptions.

Empirical results demonstrate that LaDP-FL outperforms SOTA DP-based FL methods across multiple metrics: (1) **Accuracy**: Achieves 102.99% higher accuracy on average than baselines (e.g., 236.32% over Full DP). (2) **Efficiency**: Reduces noise injection by 46.14% while mitigating privacy budget accumulation by 60.3% on average. (3) **Robustness**: Effectively thwarts reconstruction attacks, with HBC clients failing to recover private data (e.g., >12.84% increase in the FID of the reconstructed private data.).

LaDP-FL's design is agnostic to model architectures and scales efficiently with the number of clients. Future work includes extending LaDP-FL to asynchronous FL settings and further optimizing its overhead for large-scale models.

REFERENCES

- [1] B. McMahan, E. Moore, D. Ramage, S. Hampson, and B. A. y Arcas, "Communication-efficient learning of deep networks from decentralized data," in *Artificial intelligence and statistics*. PMLR, 2017, pp. 1273–1282.
- [2] S. P. Karimireddy, S. Kale, M. Mohri, S. Reddi, S. Stich, and A. T. Suresh, "Scaffold: Stochastic controlled averaging for federated learning," in *International conference on machine learning*. PMLR, 2020, pp. 5132–5143.
- [3] X. Li, K. Huang, W. Yang, S. Wang, and Z. Zhang, "On the convergence of fedavg on non-iid data," *arXiv preprint arXiv:1907.02189*, 2019.
- [4] Y. H. Ezzeldin, S. Yan, C. He, E. Ferrara, and A. S. Avestimehr, "Fairfed: Enabling group fairness in federated learning," in *Proceedings of the AAAI Conference on Artificial Intelligence*, vol. 37, no. 6, 2023, pp. 7494–7502.
- [5] B. Zhao, K. R. Mopuri, and H. Bilen, "idlg: Improved deep leakage from gradients," *arXiv preprint arXiv:2001.02610*, 2020.
- [6] W. Wei and L. Liu, "Gradient leakage attack resilient deep learning," *IEEE Transactions on Information Forensics and Security*, vol. 17, pp. 303–316, 2021.
- [7] H. Hu, X. Zhang, Z. Salcic, L. Sun, K.-K. R. Choo, and G. Dobbie, "Source inference attacks: Beyond membership inference attacks in federated learning," *IEEE Transactions on Dependable and Secure Computing*, 2023.
- [8] J. Li, M. Arazzi, A. Nocera, and M. Conti, "Subject data auditing via source inference attack in cross-silo federated learning," *arXiv preprint arXiv:2409.19417*, 2024.
- [9] B. Hitaj, G. Ateniese, and F. Perez-Cruz, "Deep models under the gan: information leakage from collaborative deep learning," in *Proceedings of the 2017 ACM SIGSAC conference on computer and communications security*, 2017, pp. 603–618.
- [10] D. Wu, J. Bai, Y. Song, J. Chen, W. Zhou, Y. Xiang, and A. Sajjanhar, "Fedinverse: Evaluating privacy leakage in federated learning," in *The twelfth international conference on learning representations*, 2024.
- [11] R. Shokri, M. Stronati, C. Song, and V. Shmatikov, "Membership inference attacks against machine learning models," in *2017 IEEE symposium on security and privacy (SP)*. IEEE, 2017, pp. 3–18.
- [12] P. Hu, Z. Wang, R. Sun, H. Wang, and M. Xue, " m^4 i: Multi-modal models membership inference," *Advances in Neural Information Processing Systems*, vol. 35, pp. 1867–1882, 2022.
- [13] C. Zhang, S. Li, J. Xia, W. Wang, F. Yan, and Y. Liu, "{BatchCrypt}: Efficient homomorphic encryption for {Cross-Silo} federated learning," in *2020 USENIX annual technical conference (USENIX ATC 20)*, 2020, pp. 493–506.
- [14] J. Ma, S.-A. Naas, S. Sigg, and X. Lyu, "Privacy-preserving federated learning based on multi-key homomorphic encryption," *International Journal of Intelligent Systems*, vol. 37, no. 9, pp. 5880–5901, 2022.
- [15] A. El Ouadhriri and A. Abdelhadi, "Differential privacy for deep and federated learning: A survey," *IEEE access*, vol. 10, pp. 22 359–22 380, 2022.
- [16] S. Truex, L. Liu, K.-H. Chow, M. E. Gursoy, and W. Wei, "Ldp-fed: Federated learning with local differential privacy," in *Proceedings of the third ACM international workshop on edge systems, analytics and networking*, 2020, pp. 61–66.
- [17] R. Xue, K. Xue, B. Zhu, X. Luo, T. Zhang, Q. Sun, and J. Lu, "Differentially private federated learning with an adaptive noise mechanism," *IEEE Transactions on Information Forensics and Security*, 2023.
- [18] X. Yuan, W. Ni, M. Ding, K. Wei, J. Li, and H. V. Poor, "Amplitude-varying perturbation for balancing privacy and utility in federated learning," *IEEE Transactions on Information Forensics and Security*, vol. 18, pp. 1884–1897, 2023.
- [19] H. Zhou, G. Yang, H. Dai, and G. Liu, "Pflf: Privacy-preserving federated learning framework for edge computing," *IEEE Transactions on Information Forensics and Security*, vol. 17, pp. 1905–1918, 2022.
- [20] J. Fu, Z. Chen, and X. Han, "Adap dp-fl: Differentially private federated learning with adaptive noise," in *2022 IEEE International Conference on Trust, Security and Privacy in Computing and Communications (TrustCom)*. IEEE, 2022, pp. 656–663.
- [21] W. Wei, L. Liu, J. Zhou, K.-H. Chow, and Y. Wu, "Securing distributed sgd against gradient leakage threats," *IEEE Transactions on Parallel and Distributed Systems*, 2023.
- [22] T. Zhang, A. Song, X. Dong, Y. Shen, and J. Ma, "Privacy-preserving asynchronous grouped federated learning for iot," *IEEE Internet of Things Journal*, vol. 9, no. 7, pp. 5511–5523, 2021.
- [23] Y. Jiang, S. Wang, V. Valls, B. J. Ko, W.-H. Lee, K. K. Leung, and L. Tassiulas, "Model pruning enables efficient federated learning on edge devices," *IEEE Transactions on Neural Networks and Learning Systems*, 2022.
- [24] Z. Jiang, Y. Xu, H. Xu, Z. Wang, C. Qiao, and Y. Zhao, "Fedmp: Federated learning through adaptive model pruning in heterogeneous edge computing," in *2022 IEEE 38th International Conference on Data Engineering (ICDE)*. IEEE, 2022, pp. 767–779.
- [25] T. Vogels, S. P. Karimireddy, and M. Jaggi, "Powersgd: Practical low-rank gradient compression for distributed optimization," *Advances in Neural Information Processing Systems*, vol. 32, 2019.
- [26] X. Ma, J. Zhang, S. Guo, and W. Xu, "Layer-wised model aggregation for personalized federated learning," in *Proceedings of the IEEE/CVF*

conference on computer vision and pattern recognition, 2022, pp. 10092–10 101.

[27] S. Lee, T. Zhang, and A. S. Avestimehr, “Layer-wise adaptive model aggregation for scalable federated learning,” in *Proceedings of the AAAI Conference on Artificial Intelligence*, vol. 37, no. 7, 2023, pp. 8491–8499.

[28] H. Hu, Z. Salcic, L. Sun, G. Dobbie, P. S. Yu, and X. Zhang, “Membership inference attacks on machine learning: A survey,” *ACM Computing Surveys (CSUR)*, vol. 54, no. 11s, pp. 1–37, 2022.

[29] K. He, X. Zhang, S. Ren, and J. Sun, “Deep residual learning for image recognition,” in *Proceedings of the IEEE conference on computer vision and pattern recognition*, 2016, pp. 770–778.

[30] A. Krizhevsky, G. Hinton *et al.*, “Learning multiple layers of features from tiny images,” 2009.

[31] K. Wei, J. Li, M. Ding, C. Ma, H. H. Yang, F. Farokhi, S. Jin, T. Q. S. Quek, and H. Vincent Poor, “Federated learning with differential privacy: Algorithms and performance analysis,” *IEEE Transactions on Information Forensics and Security*, vol. 15, pp. 3454–3469, 2020.

[32] J. Zhang, D. Fay, and M. Johansson, “Dynamic privacy allocation for locally differentially private federated learning with composite objectives,” in *ICASSP 2024-2024 IEEE International Conference on Acoustics, Speech and Signal Processing (ICASSP)*. IEEE, 2024, pp. 9461–9465.

[33] G. Yue, L. Yan, L. Kang, and C. Shen, “Adapldp-fl: An adaptive local differential privacy for federated learning,” *IEEE Transactions on Mobile Computing*, vol. 24, no. 6, pp. 5569–5583, 2025.

[34] S. Caldas, S. M. K. Duddu, P. Wu, T. Li, J. Konečný, H. B. McMahan, V. Smith, and A. Talwalkar, “Leaf: A benchmark for federated settings,” *arXiv preprint arXiv:1812.01097*, 2018.

[35] R. C. Geyer, T. Klein, and M. Nabi, “Differentially private federated learning: A client level perspective,” *arXiv preprint arXiv:1712.07557*, 2017.

[36] H. B. McMahan, D. Ramage, K. Talwar, and L. Zhang, “Learning differentially private recurrent language models,” *arXiv preprint arXiv:1710.06963*, 2017.

[37] R. Hu, Y. Guo, H. Li, Q. Pei, and Y. Gong, “Personalized federated learning with differential privacy,” *IEEE Internet of Things Journal*, vol. 7, no. 10, pp. 9530–9539, 2020.

[38] M. Kim, O. Günlü, and R. F. Schaefer, “Federated learning with local differential privacy: Trade-offs between privacy, utility, and communication,” in *ICASSP 2021-2021 IEEE International Conference on Acoustics, Speech and Signal Processing (ICASSP)*. IEEE, 2021, pp. 2650–2654.

[39] M. Yang, T. Guo, T. Zhu, I. Tjauwinata, J. Zhao, and K.-Y. Lam, “Local differential privacy and its applications: A comprehensive survey,” *Computer Standards & Interfaces*, p. 103827, 2023.

[40] H. Cai, M. Zhang, S. Wang, A. Zhao, and Y. Zhang, “Plfa-fl: Personalized local differential privacy for fair federated learning,” in *2024 27th International Conference on Computer Supported Cooperative Work in Design (CSCWD)*. IEEE, 2024, pp. 2325–2332.

[41] M. Seif, R. Tandon, and M. Li, “Wireless federated learning with local differential privacy,” in *2020 IEEE International Symposium on Information Theory (ISIT)*. IEEE, 2020, pp. 2604–2609.

[42] H. Xie, Y. Zhang, Z. Zhongwen, and H. Zhou, “Privacy-preserving medical data collaborative modeling: A differential privacy enhanced federated learning framework,” *Journal of Knowledge Learning and Science Technology ISSN: 2959-6386 (online)*, vol. 3, no. 4, pp. 340–350, 2024.

[43] B. Wang, Y. Chen, H. Jiang, and Z. Zhao, “Ppefl: Privacy-preserving edge federated learning with local differential privacy,” *IEEE Internet of Things Journal*, vol. 10, no. 17, pp. 15 488–15 500, 2023.

[44] R. Hu, Y. Guo, and Y. Gong, “Federated learning with sparsified model perturbation: Improving accuracy under client-level differential privacy,” *IEEE Transactions on Mobile Computing*, 2023.

[45] S. Chen, J. Yang, G. Wang, Z. Wang, H. Yin, and Y. Feng, “Clffd: communication-efficient layer clipping federated learning with local differential privacy,” *Journal of Systems Architecture*, vol. 148, p. 103067, 2024.

[46] X. Yang, W. Huang, and M. Ye, “Dynamic personalized federated learning with adaptive differential privacy,” *Advances in Neural Information Processing Systems*, vol. 36, pp. 72 181–72 192, 2023.

[47] X. Zhang, X. Chen, M. Hong, Z. S. Wu, and J. Yi, “Understanding clipping for federated learning: Convergence and client-level differential privacy,” in *International Conference on Machine Learning, ICML 2022*, 2022.

[48] R. Han, D. Li, J. Ouyang, C. H. Liu, G. Wang, D. Wu, and L. Y. Chen, “Accurate differentially private deep learning on the edge,” *IEEE Transactions on Parallel and Distributed Systems*, vol. 32, no. 9, pp. 2231–2247, 2021.

[49] X. Lin, J. Wu, J. Li, C. Sang, S. Hu, and M. J. Deen, “Heterogeneous differential-private federated learning: Trading privacy for utility truthfully,” *IEEE Transactions on Dependable and Secure Computing*, vol. 20, no. 6, pp. 5113–5129, 2023.

[50] M. Abadi, A. Chu, I. Goodfellow, H. B. McMahan, I. Mironov, K. Talwar, and L. Zhang, “Deep learning with differential privacy,” in *Proceedings of the 2016 ACM SIGSAC conference on computer and communications security*, 2016, pp. 308–318.

[51] C. Dwork, A. Roth *et al.*, “The algorithmic foundations of differential privacy,” *Foundations and Trends® in Theoretical Computer Science*, vol. 9, no. 3–4, pp. 211–407, 2014.

[52] Y. Zhang, M. J. Wainwright, and J. C. Duchi, “Communication-efficient algorithms for statistical optimization,” *Advances in neural information processing systems*, vol. 25, 2012.

[53] S. U. Stich, “Local sgd converges fast and communicates little,” *arXiv preprint arXiv:1805.09767*, 2018.

[54] M. D. Zeiler and R. Fergus, “Visualizing and understanding convolutional networks,” in *Computer Vision–ECCV 2014: 13th European Conference, Zurich, Switzerland, September 6–12, 2014, Proceedings, Part I 13*. Springer, 2014, pp. 818–833.

[55] J. Yosinski, J. Clune, Y. Bengio, and H. Lipson, “How transferable are features in deep neural networks?” *Advances in neural information processing systems*, vol. 27, 2014.

[56] M. Fredrikson, S. Jha, and T. Ristenpart, “Model inversion attacks that exploit confidence information and basic countermeasures,” in *Proceedings of the 22nd ACM SIGSAC Conference on Computer and Communications Security, Denver, CO, USA, October 12–16, 2015*, I. Ray, N. Li, and C. Kruegel, Eds. ACM, 2015, pp. 1322–1333. [Online]. Available: <https://doi.org/10.1145/2810103.2813677>

[57] M. Nasr, R. Shokri, and A. Houmansadr, “Comprehensive privacy analysis of deep learning: Passive and active white-box inference attacks against centralized and federated learning,” in *2019 IEEE symposium on security and privacy (SP)*. IEEE, 2019, pp. 739–753.

[58] H. Liang, Y. Li, C. Zhang, X. Liu, and L. Zhu, “Egia: An external gradient inversion attack in federated learning,” *IEEE Transactions on Information Forensics and Security*, 2023.

[59] S. Sreekumar, Z. Goldfeld, and K. Kato, “Limit distribution theory for kl divergence and applications to auditing differential privacy,” in *2023 IEEE International Symposium on Information Theory (ISIT)*. IEEE, 2023, pp. 2607–2612.

[60] L. Zang and Y. Li, “Detection and mitigation of label-flipping attacks in fl systems with kl divergence,” *IEEE Internet of Things Journal*, 2024.

[61] H. Karimi, J. Nutini, and M. Schmidt, “Linear convergence of gradient and proximal-gradient methods under the polyak-lojasiewicz condition,” in *Machine Learning and Knowledge Discovery in Databases: European Conference, ECML PKDD 2016, Riva del Garda, Italy, September 19–23, 2016, Proceedings, Part I 16*. Springer, 2016, pp. 795–811.

[62] A. Odena, C. Olah, and J. Shlens, “Conditional image synthesis with auxiliary classifier gans,” in *International conference on machine learning*. PMLR, 2017, pp. 2642–2651.

[63] A. Athalye, N. Carlini, and D. Wagner, “Obfuscated gradients give a false sense of security: Circumventing defenses to adversarial examples,” in *International conference on machine learning*. PMLR, 2018, pp. 274–283.

[64] A. Madry, A. Makelov, L. Schmidt, D. Tsipras, and A. Vladu, “Towards deep learning models resistant to adversarial attacks,” *arXiv preprint arXiv:1706.06083*, 2017.

[65] D. Zeng, S. Liang, X. Hu, H. Wang, and Z. Xu, “Fedlab: A flexible federated learning framework,” *Journal of Machine Learning Research*, vol. 24, no. 100, pp. 1–7, 2023. [Online]. Available: <http://jmlr.org/papers/v24/22-0440.html>

[66] E. J. Hu, Y. Shen, P. Wallis, Z. Allen-Zhu, Y. Li, S. Wang, L. Wang, W. Chen *et al.*, “Lora: Low-rank adaptation of large language models.” *ICLR*, vol. 1, no. 2, p. 3, 2022.

[67] Z. Chai, Y. Chen, L. Zhao, Y. Cheng, and H. Rangwala, “Fedad: A communication-efficient federated learning method with asynchronous tiers under non-iid data,” *ArXivorg*, 2020.

[68] X. Wu and C.-L. Wang, “Kafl: Achieving high training efficiency for fast-k asynchronous federated learning,” in *2022 IEEE 42nd International Conference on Distributed Computing Systems (ICDCS)*. IEEE, 2022, pp. 873–883.

[69] Y. Zhang, D. Liu, M. Duan, L. Li, X. Chen, A. Ren, Y. Tan, and C. Wang, “Fedmds: An efficient model discrepancy-aware semi-asynchronous clustered federated learning framework,” *IEEE Transactions on Parallel and Distributed Systems*, vol. 34, no. 3, pp. 1007–1019, 2023.

Supplemental Material

X. PROOF OF THEOREM 2

Due to the page limit, we only provide the proof sketch here. More details can be found in the history-revised version.

Proof Sketch of Theorem 2: Based on existing works [19], the evaluation function $f(\cdot)$ under Differential Privacy (DP) theory during neural network training is generally defined as the final model output on the corresponding training dataset. To evaluate the sensitivity within the DP framework, we need to compute the difference between the outputs of the evaluation function on two adjacent datasets and take the maximum norm of this difference across all such pairs. At this point, performing one gradient descent step on both evaluation functions $f(x)$ and $f(x')$ and subsequently applying the triangle inequality allows us to separate the gradient term from the model term. This yields the difference between the final model outputs on the two adjacent datasets at the previous epoch and the difference between their gradients at the previous epoch. For the gradient term, Assumption 1 establishes that gradients are bounded, enabling their constraint within a constant range. Consequently, we derive an iterative relationship: the sensitivity at epoch E relates to the sensitivity at epoch $E - 1$ plus a constant. Iterating this relationship back to epoch 0, where both models remain untrained on the dataset, results in identical initial outputs and zero differences. Only the accumulated gradient term, bounded by the constant term, persists. This accumulated term thus serves as the upper bound for the sensitivity within the DP framework for the model, concluding the proof.

XI. PROOF OF THEOREM 3

Due to the page limit, we only provide the proof sketch here. More details can be found in the history-revised version.

Proof Sketch of Theorem 3: Building upon the result from the book [51], we continue the derivation for the differential privacy noise of the Gaussian mechanism. Utilizing the tail bound of the Gaussian distribution for bounding, we obtain an expression consisting of a logarithmic term and a quadratic term, requiring their sum to exceed $\ln \frac{2}{\sqrt{2\pi}\delta}$. We analyze two distinct cases: $\sqrt{\frac{2}{\pi}} \leq \delta < 1$ and $0 < \delta < \sqrt{\frac{2}{\pi}}$. For the first case, the right-hand side of the constraint inequality derived from the tail bound is negative, while the quadratic term on the left-hand side is always positive. Consequently, it suffices to ensure the logarithmic term on the left is greater than zero, leading to a constrained quadratic inequality from which the result for this case readily follows. For the second case, the right-hand side of the constraint inequality is positive, necessitating a tighter bound. Under this condition, the logarithmic term on the left is readily seen to be always positive; thus, we only require the quadratic term to exceed the right-hand side. This again yields a constrained quadratic inequality, from which the result for this case is obtained. By examining these two scenarios separately, we arrive at the final conclusion of the theorem, concluding the proof.

XII. PROOF OF THEOREM 4

Due to the page limit, we only provide the proof sketch here. More details can be found in the history-revised version.

Proof Sketch of Theorem 4: We first consider the difference between the two noisy local models from adjacent rounds. Expanding one local model via gradient descent allows us to express this difference as the sum of a negative gradient term and the noise difference between the two adjacent rounds. Leveraging this insight, and invoking Assumption 2 along with the Cauchy-Schwarz inequality, we can bound the difference in the loss values of the noisy models across adjacent rounds by the sum of a gradient term, a noise term, and a cross-product term. Subsequently, based on Corollary 1, Assumption 3, and the AM-GM inequality, we further bound this difference by the squared gradient term and a constant. Reapplying Assumption 2 and subtracting the ideal optimum value F^* from both sides of the inequality allows us to relate the difference between the noisy local models and F^* at round t to that at round $t - 1$. Iterating this relationship from round 0 to round $t - 1$ demonstrates that the difference between the noisy local model at round t and F^* is bounded by the initial difference at round 0 plus a constant term. The model at round 0 is the initialization, which qualifies as a constant; hence, the upper bound on the difference between the noisy local model at round t and F^* is constrained by a constant value. Building upon this result and utilizing the aggregation process of the FedAvg strategy, we bound the difference between the global model at round t and F^* by a constant, thereby establishing the conclusion of the theorem, concluding the proof.

XIII. MATHEMATICAL SUPPORT OF THE SEQUENTIAL ACCOUNTANT METHOD IN SECTION VII-B4

The methods employed in Section VII-B4 are grounded in a fundamental theorem from the Composition Theorems of Differential Privacy theory, as illustrated in Theorem 5. The detailed proof of this theorem can be found in reference [51].

Theorem 5. *Let $\mathcal{M}_i : \mathbb{N}^{|\mathcal{X}|} \rightarrow \mathcal{R}_i$ be an $(\epsilon_i, 0)$ -DP algorithm for $i \in [k]$. Then if $\mathcal{M}_{[k]} : \mathbb{N}^{|\mathcal{X}|} \rightarrow \prod_{i=1}^k \mathcal{R}_i$ is defined to be $\mathcal{M}_{[k]}(x) = (\mathcal{M}_1(x), \dots, \mathcal{M}_k(x))$, then $\mathcal{M}_{[k]}$ is $(\sum_{i=1}^k \epsilon_i, 0)$ -Differentially Private.*

This theorem can be further extended to (ϵ, δ) -DP, as detailed in Corollary 2.

Corollary 2 (Naive Composition Theorem). *Let $\mathcal{M}_i : \mathbb{N}^{|\mathcal{X}|} \rightarrow \mathcal{R}_i$ be an (ϵ_i, δ_i) -DP algorithm for $i \in [k]$. Then if $\mathcal{M}_{[k]} : \mathbb{N}^{|\mathcal{X}|} \rightarrow \prod_{i=1}^k \mathcal{R}_i$ is defined to be $\mathcal{M}_{[k]}(x) = (\mathcal{M}_1(x), \dots, \mathcal{M}_k(x))$, then $\mathcal{M}_{[k]}$ is $(\sum_{i=1}^k \epsilon_i, \sum_{i=1}^k \delta_i)$ -Differentially Private.*

The sequential accountant method is a statistical approach based on Corollary 2. In particular, if the Gaussian noise injected during the training process satisfies the condition in Theorem 1, each noise injection step guarantees $(q\epsilon, q\delta)$ -DP, where q is the sampling probability based on the batch size. After T iterations, various advanced composition theorems can be applied to derive different privacy bounds, such as the

TABLE VI

FINAL ACCURACY PERFORMANCE OF LADP-FL AND BASELINES. “RATE” MEANS THE ACCURACY IMPROVEMENT RATE OF LADP-FL COMPARED TO EACH SOTA WORK.

Scenarios		ResNet-18@CIFAR-10					ResNet-18@CIFAR-100							
Method		LaDP-FL (Ours)	Full DP	Time-Varying DP	Sensitive DP	DPA LDP	AdapLDP	LaDP-FL (Ours)	Full DP	Time-Varying DP	Sensitive DP	DPA LDP	AdapLDP	
ϵ	0.2	Acc. (%)	77.82	58.35	63.65	64.43	66.54	73.90	41.75	10.13	22.32	29.28	36.18	38.47
	0.2	Rate (%)	-	33.37	22.26	20.78	16.95	5.30	-	312.14	87.05	42.59	15.40	8.53
	0.3	Acc. (%)	82.29	58.58	62.54	67.64	73.77	77.12	50.93	22.14	33.61	40.27	43.52	48.89
	0.3	Rate (%)	-	40.47	31.58	21.66	11.55	6.70	-	130.04	51.53	26.47	17.03	4.17
	0.4	Acc. (%)	87.12	60.71	66.79	69.68	77.94	83.28	53.42	24.18	39.13	42.39	46.75	50.86
	0.4	Rate (%)	-	43.50	30.44	25.03	11.78	4.61	-	120.93	36.52	26.02	14.27	5.03
	0.5	Acc. (%)	90.06	70.59	78.51	84.68	79.36	88.39	61.77	41.2	49.35	55.53	53.04	60.43
	0.5	Rate (%)	-	27.58	14.71	6.35	13.48	1.89	-	49.93	25.17	11.24	16.46	2.22
Average Improvement Rate		-	36.23%	24.75%	18.46%	13.44%	4.63%	-	153.26%	50.07%	26.58%	15.79%	4.99%	
Scenarios		CNN@CIFAR-10					CNN@CIFAR-100							
Method		LaDP-FL (Ours)	Full DP	Time-Varying DP	Sensitive DP	DPA LDP	AdapLDP	LaDP-FL (Ours)	Full DP	Time-Varying DP	Sensitive DP	DPA LDP	AdapLDP	
ϵ	0.2	Acc. (%)	38.81	10.00	10.00	12.23	22.97	35.79	15.69	1.23	1.87	2.87	7.73	12.04
	0.2	Rate (%)	-	288.10	288.10	217.33	68.96	8.4A	-	1175.61	739.04	446.69	102.98	30.32
	0.3	Acc. (%)	52.13	38.15	42.31	13.45	46.82	51.60	18.56	1.52	2.03	3.55	12.56	16.88
	0.3	Rate (%)	-	36.64	23.21	287.58	11.34	1.03	-	1121.05	814.29	422.82	47.77	9.95
	0.4	Acc. (%)	68.93	50.75	52.37	64.11	60.37	67.43	39.45	10.83	22.44	25.12	33.14	37.29
	0.4	Rate (%)	-	35.82	31.62	7.52	14.18	2.22	-	264.27	75.80	57.05	19.04	5.79
	0.5	Acc. (%)	75.36	63.19	69.74	71.07	70.66	76.49	40.38	22.13	28.93	35.57	35.11	39.26
	0.5	Rate (%)	-	19.26	8.06	6.04	6.65	-1.48	-	82.47	39.58	13.52	15.01	2.85
Average Improvement Rate		-	94.96%	87.75%	129.62%	25.28%	2.55%	-	660.85%	417.18%	235.02%	46.20%	12.23%	

TABLE VII

NOISE SCALE PERFORMANCE OF LADP-FL AND BASELINES. “RATE” MEANS THE NOISE REDUCTION RATE OF LADP-FL COMPARED TO EACH SOTA WORK.

Scenarios		ResNet-18@CIFAR-10					ResNet-18@CIFAR-100							
Method		LaDP-FL (Ours)	Full DP	Time-Varying DP	Sensitive DP	DPA LDP	AdapLDP	LaDP-FL (Ours)	Full DP	Time-Varying DP	Sensitive DP	DPA LDP	AdapLDP	
ϵ	0.2	Noise Scale	275,447	727,901	862,998	242,583	386,453	735,138	302,859	787,542	532,786	281,766	379,128	762,930
	0.2	Rate (%)	-	62.16	68.08	-13.55	28.72	62.53	-	61.54	43.16	-7.49	20.12	60.30
	0.3	Noise Scale	132,365	505,266	295,231	165,234	261,698	512,366	167,884	543,256	324,836	127,458	274,038	538,719
	0.3	Rate (%)	-	73.80	55.17	19.89	49.42	74.17	-	69.10	48.32	-31.72	38.74	68.84
	0.4	Noise Scale	87,563	383,945	224,129	95,468	241,778	402,970	101,256	436,562	192,879	97,145	239,767	399,175
	0.4	Rate (%)	-	77.19	60.93	8.28	63.78	78.27	-	76.81	47.50	-4.23	57.77	74.63
	0.5	Noise Scale	51,658	203,968	193,487	53,997	156,947	217,344	94,253	267,569	122,365	88,766	142,834	232,067
	0.5	Rate (%)	-	74.67	73.30	4.33	67.09	76.23	-	64.77	22.97	-6.18	34.01	59.39
Average Reduction Rate		-	71.96%	64.37%	4.74%	52.25%	72.80%	-	68.06%	40.49%	-12.40%	37.66%	65.79%	
Scenarios		CNN@CIFAR-10					CNN@CIFAR-100							
Method		LaDP-FL (Ours)	Full DP	Time-Varying DP	Sensitive DP	DPA LDP	AdapLDP	LaDP-FL (Ours)	Full DP	Time-Varying DP	Sensitive DP	DPA LDP	AdapLDP	
ϵ	0.2	Noise Scale	21,747	61,523	44,752	22,754	31,052	63,489	22,968	77,523	50,803	23,854	35,603	72,781
	0.2	Rate (%)	-	64.65	51.41	4.43	29.97	65.75	-	70.37	54.79	3.71	35.49	68.44
	0.3	Noise Scale	15,870	48,236	30,983	17,038	24,647	45,913	19,297	52,652	34,114	21,271	37,329	56,700
	0.3	Rate (%)	-	67.10	48.78	6.86	35.61	65.43	-	63.35	43.43	9.28	48.31	65.97
	0.4	Noise Scale	8,798	34,717	18,156	9,047	14,029	36,140	9,028	42,236	23,578	9,548	27,668	44,469
	0.4	Rate (%)	-	74.66	51.54	2.75	37.29	75.66	-	78.62	61.71	5.45	67.37	79.70
	0.5	Noise Scale	7,166	19,852	11,549	8,378	9,033	20,149	8,677	25,786	18,270	8,933	10,119	18,574
	0.5	Rate (%)	-	63.90	37.94	14.47	20.67	64.43	-	66.35	52.51	2.87	14.25	53.28
Average Reduction Rate		-	67.58%	47.42%	7.12%	30.88%	67.82%	-	69.68%	53.11%	5.33%	41.35%	66.85%	

$(qT\epsilon, qT\delta)$ -DP. This framework allows a rigorous quantification of privacy guarantees in iterative training processes under differential privacy.

The detailed quantitative steps of the sequential accountant method used in Section VII-B4 are as follows:

- 1) Determine the specific privacy budget consumed by the algorithm during the protection process by deriving the actual variance of the injected noise distribution.

$$\sigma = \sqrt{2 \log \frac{1.25}{\delta}} / \epsilon. \quad (17)$$

- 2) Determine the q by the batch size of the training process.

$$q = \frac{\text{Batch_Size}}{|\mathcal{D}_i|}. \quad (18)$$

- 3) Determine the iteration number T .

- 4) Determine the cumulative privacy budget by the sequential accountant method.

$$O(\epsilon) = qT\epsilon. \quad (19)$$

XIV. MORE EXPERIMENTAL RESULTS

We present all the numerical results of LaDP-FL and SOTA works (including Full DP, Time-Varying DP, and Sensitive DP) across all experimental scenarios. Table VI shows the final accuracies of each method under different scenarios as well as the accuracy improvement rates of LaDP-FL compared to SOTA works. Table VII shows the total noise scales of each

TABLE VIII
STATISTICAL SIGNIFICANCE (P-VALUES) OF DIFFERENT METRICS BETWEEN LADP-FL AND BASELINES.

Metrics	Scenario	Full DP	Time-Varying DP	Sensitive DP	DPA LDP	AdapLDP
Accuracy	ResNet-18@CIFAR-10	1.54e-6	2.64e-5	4.61e-5	3.02e-4	4.23e-2
	ResNet-18@CIFAR-100	1.86e-6	2.64e-5	1.67e-2	2.26e-2	1.27e-1
	CNN@CIFAR-10	2.73e-3	1.93e-2	3.74e-2	2.35e-2	5.34e-2
	CNN@CIFAR-100	3.21e-4	9.35e-3	7.34e-3	5.91e-3	7.97e-2
	Average	7.64e-4	7.18e-3	1.54e-2	1.31e-2	7.56e-2
Noise scale	ResNet-18@CIFAR-10	2.20e-6	3.19e-4	5.59e-1	2.73e-3	2.20e-6
	ResNet-18@CIFAR-100	2.20e-6	2.27e-3	2.35e-1	1.67e-2	2.20e-6
	CNN@CIFAR-10	2.64e-5	2.49e-3	2.83e-1	2.04e-2	2.24e-5
	CNN@CIFAR-100	1.54e-6	5.64e-4	3.37e-4	3.19e-4	2.38e-4
	Average	8.09e-6	1.41e-3	3.54e-1	1.01e-2	6.62e-5
Accumulative privacy budget	ResNet-18@CIFAR-10	2.64e-5	2.24e-6	3.49e-3	4.67e-6	2.64e-5
	ResNet-18@CIFAR-100	2.64e-5	1.54e-6	1.85e-2	1.86e-6	2.64e-5
	CNN@CIFAR-10	2.64e-5	5.58e-6	3.64e-2	3.24e-6	2.64e-5
	CNN@CIFAR-100	2.64e-5	1.55e-6	3.32e-2	6.68e-6	2.64e-5
	Average	2.64e-5	2.73e-6	2.29e-2	4.11e-6	2.64e-5

* All p-values were computed based on experimental data from the final five rounds. For each algorithm and scenario, the final five rounds of data were selected to enhance statistical power and reliability, thus mitigating the risk of failing to detect genuine differences due to very small sample sizes.

method under different scenarios as well as the reduction ratios of LaDP-FL compared to SOTA works.

Based on Table VI, we can calculate the average improvement rate of LaDP-FL compared to each SOTA work. Using the average improvement rate compared to Full DP as an example, we averaged all the average improvement rates across all experimental scenarios as follows:

$$(36.23\% + 153.26\% + 94.96\% + 660.85\%) / 4 = 236.32\%, \quad (20)$$

which is consistent with the value in the Introduction.

Similarly, we have the average improvement rate compared to Time-Varying DP, Sensitive DP, DPA LDP, and AdapLDP as 144.93%, 102.42%, 25.18%, and 6.10%. Then, we averaged the improvement rates of these three algorithms to obtain the overall average improvement value:

$$(236.32\% + 144.93\% + 102.42\% + 25.18\% + 6.10\%) / 5 = 102.99\%. \quad (21)$$

We can calculate the average noise reduction rate with the same method based on Table VII. Using the average reduction rate compared to Full DP as an example, we averaged all the average reduction rates across all experimental scenarios as follows:

$$(71.96\% + 68.06\% + 67.58\% + 69.68\%) / 4 = 69.32\%, \quad (22)$$

which is consistent with the value in the Introduction.

Similarly, we have the average reduction rate compared to Time-Varying DP, Sensitive DP, DPA LDP, and AdapLDP as 51.35%, 1.20%, 40.54%, and 68.31%. Then, we averaged the reduction rates of these three algorithms to obtain the overall average reduction value:

$$(69.32\% + 51.35\% + 1.20\% + 40.54\% + 68.31\%) / 5 = 46.14\%. \quad (23)$$

We present the results of the statistical significance (p-values) of prediction accuracy comparisons, noise scale comparisons, and cumulative privacy budget comparisons between LaDP-FL and baselines in Table VIII.

TABLE IX
ACCURACY AND TRAINING DURATIONS PERFORMANCE OF LADP-FL AND BASELINES WHEN TRAINING RESNET-152 ON CIFAR-100.

Method		LaDP-FL (Ours)	Full DP	Time-Varying DP	Sensitive DP	DPA LDP	AdapLDP
$\epsilon = 0.2$	Acc. (%)	82.44	45.18	62.99	68.43	72.05	75.31
	Duration (s)	257,104	239,816	242,993	247,302	254,731	263,998
$\epsilon = 0.5$	Acc. (%)	89.40	72.33	77.59	74.81	83.57	86.12
	Duration (s)	256,943	239,407	243,434	247,759	254,003	265,376

TABLE X
THE COMPARATIVE QUALITY OF PRIVACY DATA GENERATION BY ADVERSARIES WHEN CONFRONTING LADP-FL VERSUS BASELINE PRIVACY-PRESERVING ALGORITHMS ACROSS DIVERSE PRIVACY DATA TYPES.

Privacy Budget	Method	FID score across diverse labels				
		car	horse	bird	A	e
0.2	No protection	33.98	40.16	52.77	21.93	17.40
	Full DP	79.14	77.38	144.62	47.95	44.14
	Time-Varying DP	67.89	69.13	108.37	39.22	30.15
	Sensitive DP	70.44	78.86	139.02	47.37	43.99
	DPA LDP	58.44	59.30	119.79	36.35	31.44
	AdapLDP	42.37	48.29	79.36	33.63	34.52
	LaDP-FL	68.33	72.79	147.22	34.80	28.66
0.5	Full DP	49.33	42.07	76.68	26.79	28.40
	Time-Varying DP	51.29	43.33	67.92	24.57	25.88
	Sensitive DP	53.77	50.98	81.49	34.05	33.91
	DPA LDP	46.25	45.58	62.46	22.73	21.99
	AdapLDP	39.42	44.41	55.72	20.80	24.39
	LaDP-FL	46.79	48.03	94.82	27.74	37.46

* The FID scores are computed based on 10,000 adversarially reconstructed privacy images per label, with all tabulated experimental results representing averages derived from three independent runs.

* Higher FID scores indicate greater semantic incoherence in generated images, signifying enhanced privacy protection performance that effectively prevents adversaries from successfully reconstructing private data.

The experimental results of the ResNet-152 are presented in Table IX, demonstrating the scalability of LaDP-FL on the deep model.

Table X presents the FID scores when confronting the LaDP-FL's defense and baselines' defense mechanisms, illustrating the quality of the reconstructed privacy data, thereby showcasing the protection capabilities of LaDP-FL and baselines.